Influence of the Radial Magnetic Field of a SONA Transition Unit on Polarization of Particles
- Bachelor Thesis -

Nils Michael Hanold
Matrikel-Nr.: 2627863
nils.hanold@hhu.de

Faculty of Mathematics and Natural Sciences of
Heinrich-Heine-University Düsseldorf

October 2023

First examiner: Prof. Dr. Markus Büscher
Second examiner: Prof. Dr. Dr. Carsten Müller

Abstract

The capability of a Sona transition unit to induce transitions between the different hyperfine states of atoms is known from [1], [2] and [5]. The specific transition that is induced depends on the longitudinal and the radial magnetical fields of the transition unit.
Performed simulations of the occupation numbers of different Hydrogen hyperfine substates show that also the radial distance of the atomic beam from the beam axis to the edge of the coils seems to be important, because the radial magnetic field amplitude is rising from the center of a magnetic coil to the edge.
This predicted behavior was proofed by measurements with a new type of a Sona transition unit that was constructed and build for this thesis. One important result was that more particles take part in the hyperfine transitions inside the Sona unit by using radial offsets from the beam axis. This results in larger amplitudes of the oscillation between a high populated and high depolulated state while increasing the current inside the Sona unit. The measurements show that especially at small magnetic fields the amplitudes of the oscillations for one hyperfine state is increasing with an increasing radial offset from the beam axis.
It was also possible to increase the amplitudes of these oscillations of the hyperfine states from an unpolarized atom beam by using a radial offset. Therefore, it is possible to polarize an unpolarized particle beam by using — in the laboratory frame — static magnetic fields. This is an improvement of the known possibilities to create a polarized particle beam because of the comparatively easy and cheap way to produce and build these devices instead of other methods.

Zusammenfassung

Dass mit einer Sona Übergangseinheit Übergänge innerhalb der Hyperfeinstruktur eines Atoms induziert werden können, ist aus [1], [2] und [5] bekannt. Der jeweilige Übergang, der induziert wird, hängt dabei von den longitudinalen und radialen Magnetfeldern der Übergangseinheit ab.
Simulationen der Besetzungswahrscheinlichkeiten der Hyperfeinstruktur-Zustände zeigen, dass der radiale Abstand des Atomstrahls von der Strahlachse einen signifikanten Einfluss auf auf die Polarisation der Atome hat. Das kann damit erklärt werden, dass das radiale Magnetfeld mit zunehmendem Abstand von der Strahlachse ansteigt.
Dieses Verhalten wurde durch Messungen mit einer eigens dafür konzipierten SONA Übergangseinheit untersucht und durch Messungen bestätigt. Eine wichtige Erkenntnis war, dass mit zunehmendem radialen Abstand des Atomstrahls von der Strahlachse die Amplitude der Oszillationen zwischen einem hoch besetzten und einem schwach besetzten Zustand zunehmen und damit mehr Atome von den induzierten Übergängen in der Hyperfeinstruktur betroffen sind. Das hat einen direkten Einfluss auf die zu erreichende Polarisation des Atomstrahls, welche dadurch ebenfalls mit einem größeren radialen Abstand von der Strahlachse zunimmt.
Dieses Verhalten ist ebenfalls bei Benutzung eines nicht vorpolarisierten Atomstrahls zu beobachten, was die Möglichkeit eröffnet, nur unter Benutzung von — im Laborsystem — statischen Magnetfeldern effektiv Polarisation in einem einfallendem Atomstrahl zu erzeugen. Aufgrund der im Vergleich zu andern Polarisationsmethoden einfachen Bauweise und Handhabung der Übergangseinheit, bietet sich eine Benutzung zur Erzeugung von polarisierten Atomstrahlen an.

Contents

List of Figures

1 Introduction

The scattering cross section of a particle is a measure for the possibility of a — arbitrary — force interaction with other objects. With a higher cross section an interaction of the observed objects is more likely [3].
The cross section of the nuclear fusion reaction is depending on the spins of the particles and their orientation to each other [4]. To be able to control the spins of the particles would mean to have the ability to manipulate the probability of a fusion reaction. To archieve this goal and make it useful for future experiments and applications a reliable method to polarize the fuel is needed. The spin polarization of particles is already possible but usually not without complex and expensive methods.
An easy and cheap method to emerge a polarized particle beam is the use of a Sona transition unit [1]. This device was invented to switch the electron polarization of an atomic hydrogen beam, induced either by optical pumping with lasers or by selective quenching of metastable atoms, into a nuclear polarization. This happens when hydrogen atoms with electron and nuclear spin parallel to an external field move through a zero crossing. By that the quantization axis can be rotated faster than the spin can follow and, thus, afterwards both spins are antiparallel to the quantization axis.

In 2007 a team of the Brookhaven National Laboratory presented their observations of oscillating occupation numbers of the hyperfine substates within a Hydrogen beam while using a Sona unit with improved magnetical fields at 'The International Workshop of Polarized Ion Sources, Targets and Polarimeter' [2].

In 2021 the work was continued at the *Nuclear Physics Institute* at the Forschungszentrum Jülich and both, measurements and simulations of the occupation numbers of the hyperfine states for a Hydrogen atomic beam were performed. They showed clear visible oscillations between the different states if specific magnetic field shapes were used [5].
In this thesis an option is described which allows to emerge a polarized beam out of an unpolarized beam and the influence of one magnetical field component that is responsible for this interaction:
Simulations for the occupation numbers of the hyperfine states showed a clear visible increase for the grade of polarization and, therefore, for the amount of atoms that take part on the photon interactions.
The idea for this thesis was in best case to verify the simulations or otherwise to disprove it.

2 Theory

2.1 Atom Models and Coupling

The idea for a model of atoms is thousands of years old. In the early 20$^{\text{th}}$ century atomic models were developed which are similar to such we use nowadays. Starting comparatively simple with the 'plum pudding model' in 1904 by J.J. Thomson, some adoptions by other physicans in the following years, the 'Rutherford model' by E. Rutherford and the 'Bohr model of atoms' by N. Bohr in 1913 which was the main inspiration for following improvements and models [3].

It postulates that the movement of electrons is only allowed on defined orbits where they do not emit radiation. Every orbit stands for a discrete value of binding energy that is allowed on this orbit:

$$E_{\mathrm{n}} = -R\,h\,c\,\frac{1}{\mathrm{n}^2} \qquad [3] \qquad (2.1)$$

With the Rydberg constant R, the Planck constant h, the speed of light c and n is the number of the orbit.
The first orbit or atomic shell is the n = 1 shell. Starting with this atomic shell all additional electrons are placed as allowed by the Pauli exclusion principle until the shell is filled. If an electron changes to higher orbits the energy difference must be overcome while an orbit change to lower orbits will emit this energy difference in form of a photon.

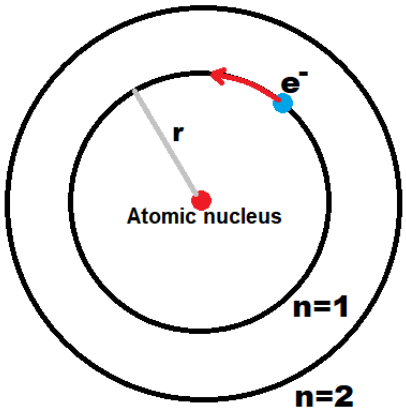

Figure 2.1: Bohr model of atoms.

The movement of the electron itself can be understood as a circulating charge with a known mass. Each moving mass has an angular momentum that is perpedicular to the plane of the movement. The circulating charge causes a magnetic field, and thus a magnetic moment that is pointing in the opposide direction of the angular momentum [3].

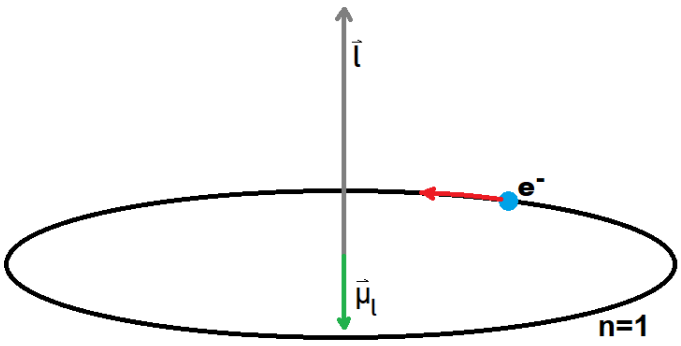

Figure 2.2: Angular momentum of the electron.

In 1921 O. Stern and W. Gerlach performed an experiment to investigate the behavior of silver atoms in an inhomogeneous magnetic field [3].
They used a furnace to emerge silver atoms in the groundstate and let them pass an inhomogeneous magnetic field. Their expectation for this experiment was to see a continuous emerging spectra which could be detected by a glass-screen, but instead they observed that the beam splits up into two different beams. Thus, they discovered against their expectations the spin of the electrons.

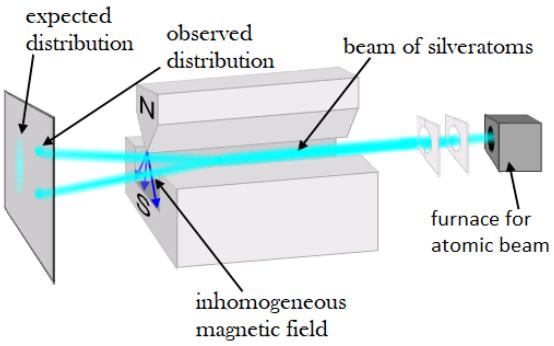

Figure 2.3: Stern-Gerlach-experiment [F1].

The explanation for this behavior nowadays is that the outermost electron of the silver atom in the groundstate is in the $5S_{1/2}$ state with an angular momentum of $l = 0$ so the main influence on the magnetic moment of the atom is caused by the spin of the electrons because the spin of the nucleous can be neglected. Furthermore, it was the first proof that the electron spin, and thus, the magnetic moment of the electron is quantized in two directions.

The reason for this result was the spin of the electrons that is causing another magnetic moment which is antiparallel to the spin and triggers a force to the higher magnetic field inside of inhomogeneous magnetic fields.
The mentioned angular momentum that an electron has because of its movement on an orbit couples with the electron spin to the total angular momentum of the electrons $\vec{j} = \vec{l} + \vec{s}$ [3]:

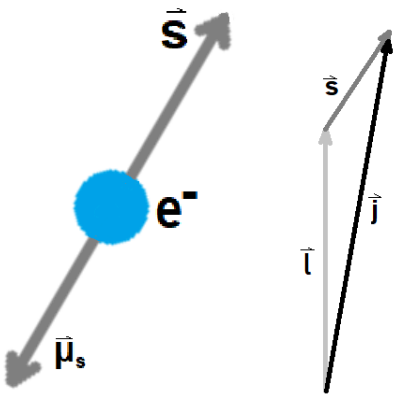

(a) (b)

Figure 2.4: Magnetical projection of the electron spin and total angular momentum of electrons.

The sum of the angular momenta of all electrons in case of a multi-particle system is named J. This combination of electron spin and angular momentum of the electron describes the *fine structure* of the atom.

Like an electron also the nucleus of an atom has got a magnetic moment which can be understood as another spin, named I [6]. This spin is induced by the spins of the nucleons — the protons and neutrons — neglecting that the nucleons have a substructure build up with fermions, the up- and down-quarks.

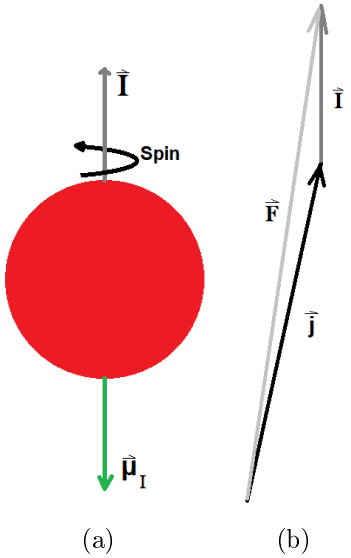

Figure 2.5: Total Angular momentum of the atom.

The spin of the nucleus couples with the total spin of the electrons to the main angular momentum of the atom [6]

$$\vec{F} = \vec{J} + \vec{I}. \tag{2.2}$$

The quantum number F describes the whole magnetic moment of the atom and is considered in the *hyperfine structure*.

The different possibilities for the coupling of spin, angular momentum and the nucleus spin cause a degeneration of energy. Every magnetic moment of the atom and the relative position to each other is an additional contribute to the potential energy — even if it only appears in external magnetic fields.

In the Bohr model the energy levels are fully degenerated. Every additional coupling of the spin or the angular momentum has got an influence on the energy level and strength of the split up. The different energy levels of the different possibilities for coupling are shown in Fig.2.6.

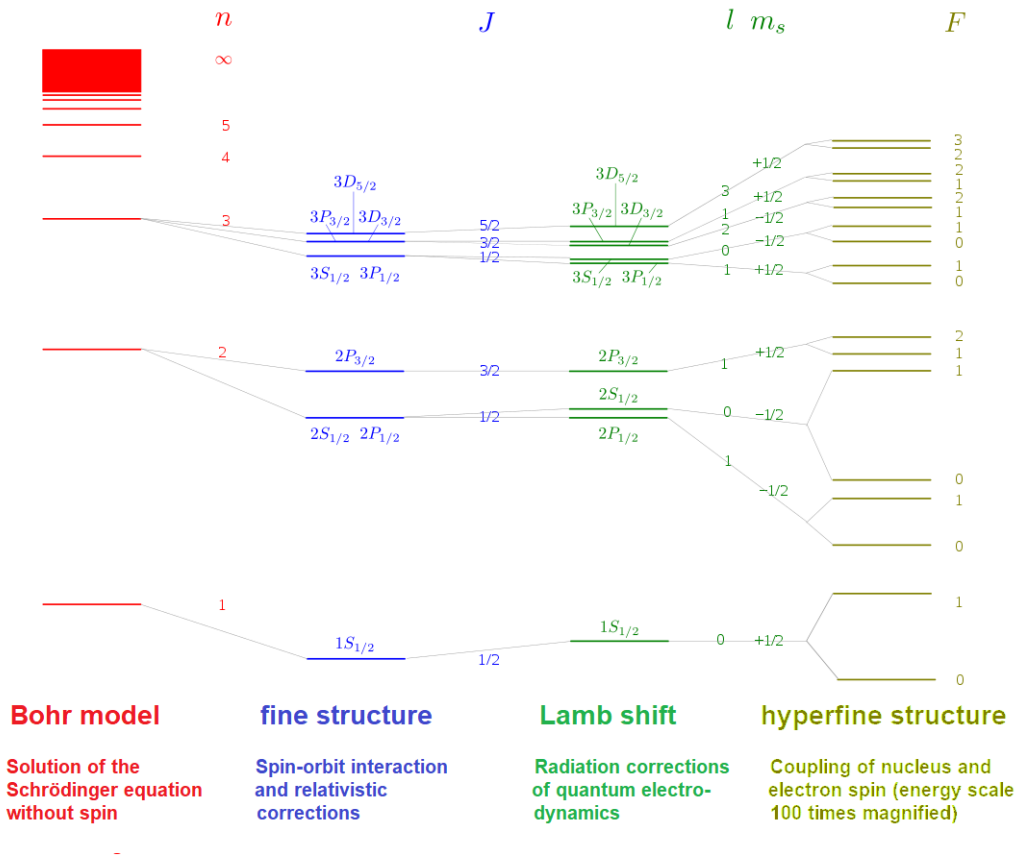

Figure 2.6: Energy corrections of the hydrogen eigenenergies [F2].

The coupling of the nucleus and electron spins can be found in the hyperfine structure section on the right side. The Lamb-shift is an effect from the QED (**q**uantum **e**lectro**d**ynamics) that considers the quantum fluctuation of the electron while its movement on the orbit.

2.2 Behavior within External Fields

The magnetic moments of the atoms align themself inside of an external magnetic field and the main magnetic moment of an atom precesses around the magnetic field lines, the so called quantization axis [3]. In a homogenous magnetic field a magnetic dipole receives an angular momentum and, thus, an additional potential energy in this field.
The different energy levels of the hyperfine structure are raising in external magnetic fields and split up even more because of the additional potential energy they receive due to the interaction with an external magnetic fields.

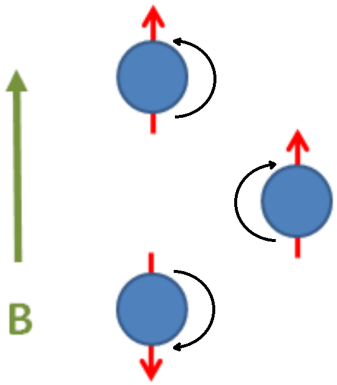

Figure 2.7: Alignment in an external magnetic field [F3].

Depending on the orientation of the spins inside the atom the energy levels are developing differently within external magnetic fields and are called Breit-Rabi states hereafter.
The energies of the Breit-Rabi states are described by the eigenenergies of the states like shown in [7]. The eigenenergies of a hydrogen atom within external magnetic fields are the solution of the eigenproblem for this system and are determined as

$$\begin{aligned}
\mathrm{E}_1 &= \alpha_1 = \frac{\mathrm{A_{H,2S}}}{4} - \frac{1}{2}(g_J\mu_B + g_I\mu_N)B \\
\mathrm{E}_2 &= \alpha_2 = -\frac{\mathrm{A_{H,2S}}}{4} + \frac{1}{2}\sqrt{\mathrm{A}^2_{\mathrm{H,2S}} + (g_J\mu_B - g_I\mu_N)^2B^2} \\
\mathrm{E}_3 &= \beta_3 = \frac{\mathrm{A_{H,2S}}}{4} + \frac{1}{2}(g_J\mu_B + g_I\mu_N)B \\
\mathrm{E}_4 &= \beta_4 = -\frac{\mathrm{A_{H,2S}}}{4} - \frac{1}{2}\sqrt{\mathrm{A}^2_{\mathrm{H,2S}} + (g_J\mu_B - g_I\mu_N)^2B^2}.
\end{aligned} \tag{2.3}$$

With $\mathrm{A_{H,2S}}$ as the hyperfine structure constant of a Hydrogen atom in the exited $2S_{1/2}$ state, g_J and g_I are the g factors of the electron and proton, μ_B is the Bohr magneton and μ_N the nuclear magneton.
The derivation of this formulas can be found in [7].

The behavior of the Breit-Rabi states is shown in the Breit-Rabi diagram in fig. 2.8 for a H atom in the exited $2S_{1/2}$ state:

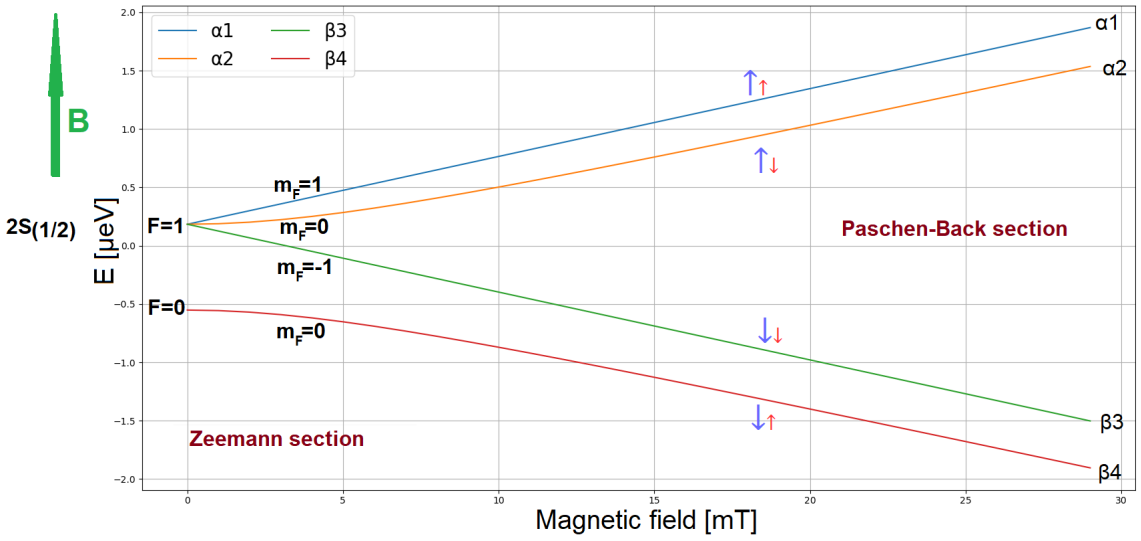

Figure 2.8: Breit-Rabi diagram for or H_1 in an excited $2S_{1/2}$ state.

For magnetic field strengths below $\mathrm{B_c} = 6.34\,\mathrm{mT}$ the spins of the nucleus and the electron can be seen as coupled to the total angular momentum of the atom F. This area is called the Zeemann-section. The magnetic projection m_F varies between $-F$ and F [6]. For $F = 1$ there are three substates $m_F = -1, 0, 1$, named here α_1, α_2 and β_3. For $F = 0$ there is the $m_F = 0$ substate, called β_4. With higher magnetic fields the influence of the different spin orientation is increasing, and thus, the energy levels are changing continually.

At higher magnetic fields above $B_c = 6.34\,mT$ the Zeemann-section is devolving to the Paschen-Back section. In this area the induced energy by the external magnetic field exceeds the magnetic coupling energy of the spins and, thus, the spins are decoupling and precess around the quantization axis individually. Beside the states the electron and nucleus spins are marked: blue colored for the electron and red for the nucleus spin.
In this experiment the non constant rising energy difference between the α_1 and α_2 state is used as well as the approximately constant rising energy difference between the α_2 and β_3 hyperfine substate.

Another effect that is appearing in this experiment in the so called *'hyperfine beat'* [8]. This interaction is an appearance of the α_2 and β_4 states which are sharing the same states except their symmetry. Thus they can change into the other state and back again which results in an oscillation of these two states just by their equal hyperfine state numbers.

2.3 Theory for a Transition Unit

In 1967 P.G. Sona published a paper and described a method to polarize a particle beam with a transition unit. The device that is called by his inventor 'Sona' unit has the task to provide a magnetic field with a zero crossing in the middle of the device which causes the exchange of an electron-polarized into a nuclear-polarized beam by changing the quantization axis 'fast' enough, so the spin of the particles can not precess around the changing axis and 'flip' into the other state [1]:

$$\omega_B >> \omega_{Larmor}. \tag{2.4}$$

The 'frequency' of the changing magnetic field is given by the velocity of the particles v and the distance it experience the magnetic field $\frac{\lambda}{2}$. For a longitudinal magnetic field along the z-axis the conditions are given by:

$$\frac{2 \cdot v}{\lambda} >> \mu_e \cdot B_{radial} = \frac{e}{2 \cdot m_e} \cdot \frac{\partial B_{longitudinal}}{\partial z} \cdot \frac{r}{2}. \tag{2.5}$$

So the required change of the longitudinal magnetic field can be determined to:

$$B'_z << \frac{8 \cdot v \cdot m_e}{e \cdot r \cdot \lambda}. \tag{2.6}$$

The required magnetic field shape (Fig. 2.9) is provided by magnetic field coils.

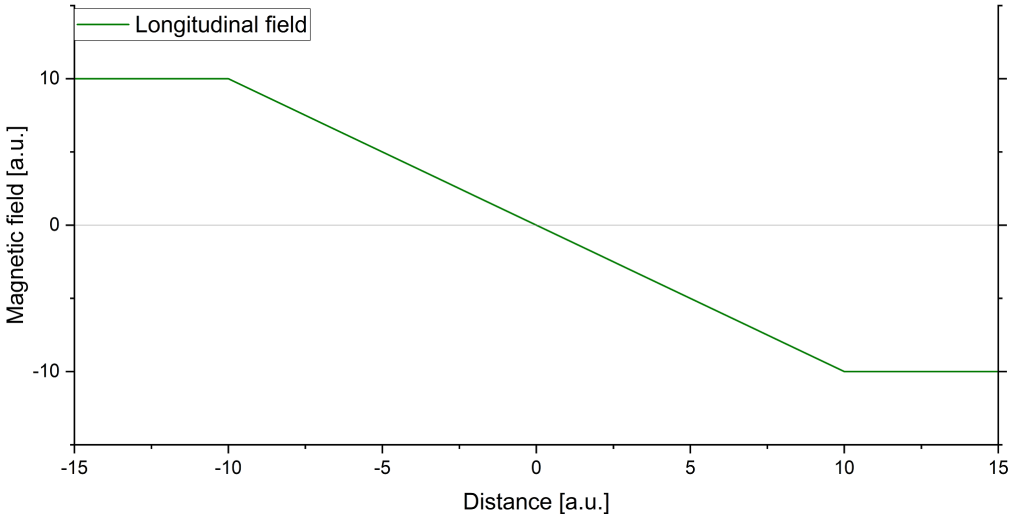

Figure 2.9: Longitudinal magnetic field of a 'classical' Sona unit.

The behavior of the hyperfine states of an atom which passes the transition unit can be seen very well if the Breit-Rabi diagram is extended to negative fields (Fig. 2.10).

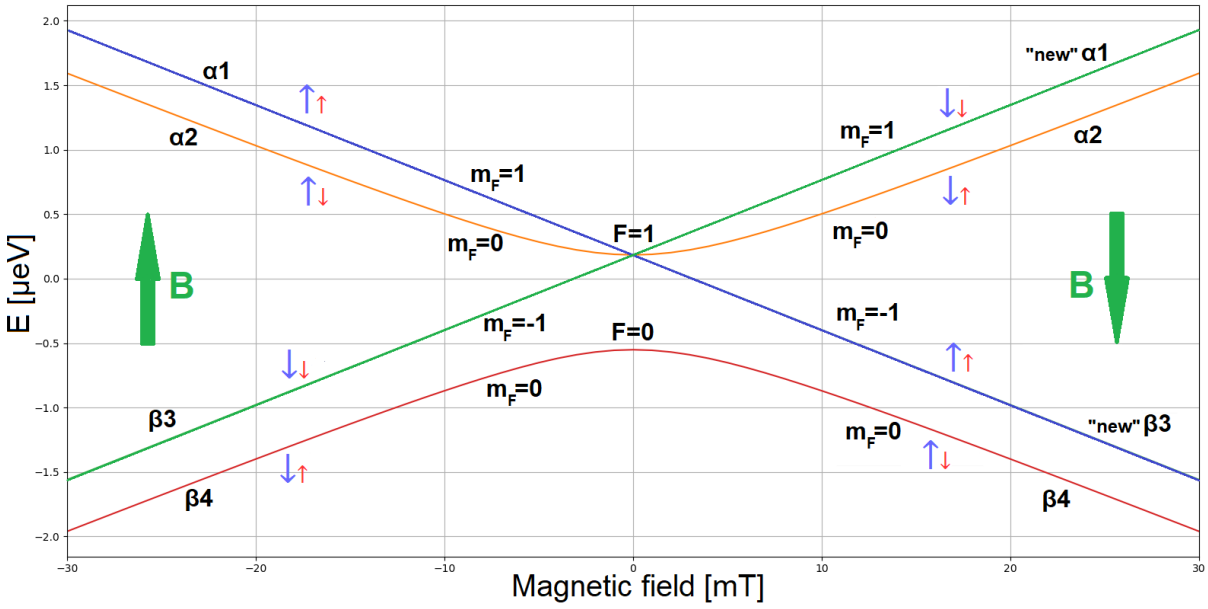

Figure 2.10: Breit-Rabi diagram for extended magnetic fields.

The zero crossing of the longitudinal magnetic field is in the middle of the Sona unit at 0 mT and changes the quantization axis of the particles immediately which is causing — by definition — the 'flip' of some particles into other states: The α_1 state, with electron and nuclear spin parallel to the external field, is now the 'new' β_3 state and the other way around. The α_2 and β_4 states remain the same [1],[5].

Performed experiments at the Brookhaven National Laboratory in 2007 showed that with specially shaped magnetic fields additional transitions can be induced than only with constant longitudinal magnetic fields like in the 'classical' Sona transition unit. An oscillation of a high populated to a high depolpulated state was observed but could not be explained in detail.
In 2021 a new type of Sona transition unit was invented [5] with sinusodial shaped magnetic fields (Fig. 2.11, green graph). The radial magnetic field (Fig. 2.11, orange graph) of this type of field shape is able to induce photon transitions betweeen the hyperfine substate of an incoming atom.

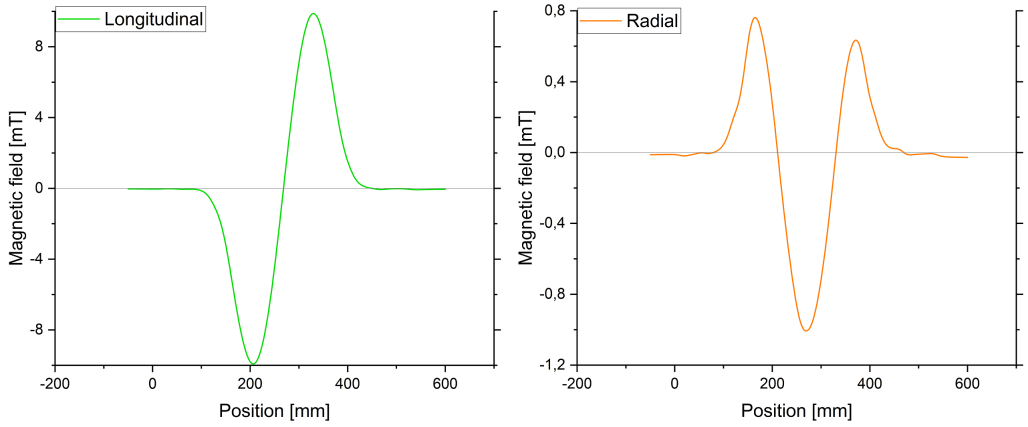

(a) (b)

Figure 2.11: Longitudinal and radial magnetic field of a specific Sona unit (B_z and B_r in cylinder coordinates) [9].

In the laboratory frame the Sona unit has a static magnetic field with a zero crossing for the turn of the quantization axis between the coils. In the inertial system of the atoms the magnetic field of the Sona unit is no longer seen as a static magnetic field. The incoming atoms will see not only a magnetic field changing in time [5], but according to the Maxwell-Faraday equation also an electric field [10]. So the static radial magnetic field is experienced as an electromagnetic wave that is able to induce transitions between the hyperfine states if the seen wavelength fits to the required energy.

If this energy or — because of the conservation of the angular momentum — an odd multiply of it fits between the distances of the hyperfine states a transition is induced [5]. Because of the different slopes of the energy levels the transitions of $\alpha_1 \leftrightarrow \alpha_2$ and $\alpha_2 \leftrightarrow \beta_3$ take place at differnt areas for the magnetic field amplitudes at the Breit-Rabi diagram (Compare fig. 2.12). The difference of the energy levels for the $\alpha_1 \leftrightarrow \alpha_2$ transition is rising with higher magnetic fields but the raise becomes less until the energy levels are developing parallel, due to the fact that the energy level of α_2 is not evolving linear. The distance of the $\alpha_2 \leftrightarrow \beta_3$ energy levels is increasing more and more with higher magnetic fields.

The most transitions induced by the radial magnetic field take place between the $\alpha_1 \leftrightarrow \alpha_2$ and $\alpha_2 \leftrightarrow \beta_3$ states. The fourth state, β_4 is too far away in the energetic scale

so photon transitions are non likely and the only influence by it is the hyperfine beat with the α_2 state [8].

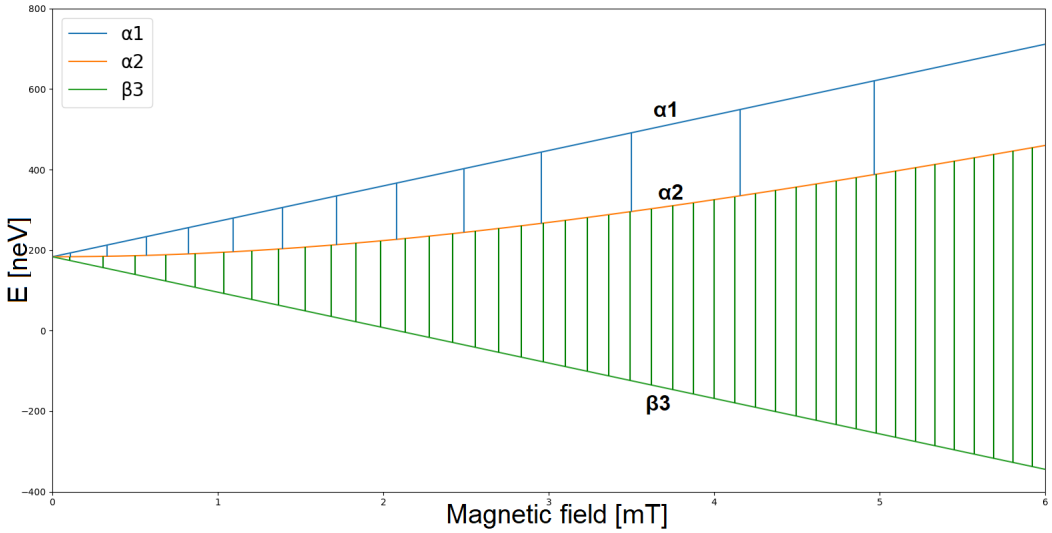

Figure 2.12: Breit-Rabi diagramm with cross sections for transitions.

If the current inside the transition unit is increased the repetition rate of the $\alpha_1 \leftrightarrow \alpha_2$ transitions becomes slower with higher magnetic fields and are called the *'slow'* transitions hereafter. The repetition rate of the $\alpha_2 \leftrightarrow \beta_3$ transitions becomes faster and are called the *'fast'* transitions in this thesis. The β_4 state is not marked because the distance of the energy levels is too large to make a transition likely.

To analyse the transitions of the Sona unit two different theories can be used: The photon model and the so called *wave model* which representates the mathematical describtion of this behavior.

2.4 Photon Model

Applying the photon model the Breit-Rabi state transition by the radial magnetic field can be understood as a photon induced transition: The electromagnetic wave caused by the radial magnetic field can be seen as a wave with $1\,\frac{1}{2}$ oscillations, and thus, it can be seen like two different photons which are sharing the middle part of the oscillation [11].

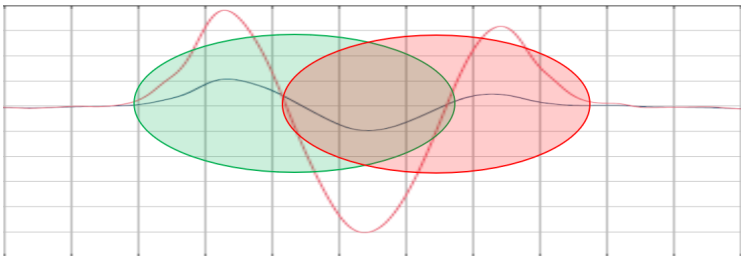

Figure 2.13: Radial magnetic field with virtual photons [P1].

These virtual photons can be absorbed by the incoming atoms and induce transitions between the Breit-Rabi states.

A common measurement with one of the former Sona units was the so called 'α_1 to α_1 spectra'. Both spin filters are filtering for α_1 while increasing the magnetic field of the Sona unit constanty. That means that only atoms in the α_1 state are detected as a signal, because after the zero crossing of the longitudinal magnetic field all α_1 atoms should be in the β_3 state due to the 180 ° turn of the quantization axis. The only positive influence on the measured signal are the induced transitions by the radial magnetic field of the Sona unit. In this case the incoming particle would absorb a photon on the left side of the zero crossing of the longitudinal field (Fig. 2.15, left side, green arrow down), switch into the α_2 state, cross the Sona unit without a change of the Breit-Rabi state and again absorb a photon to switch back into the α_1 state (Fig. 2.15, right side, green arrow up). All other particles that are not absorbing a photon will switch into the β_3 state by the turn of the quantization axis.

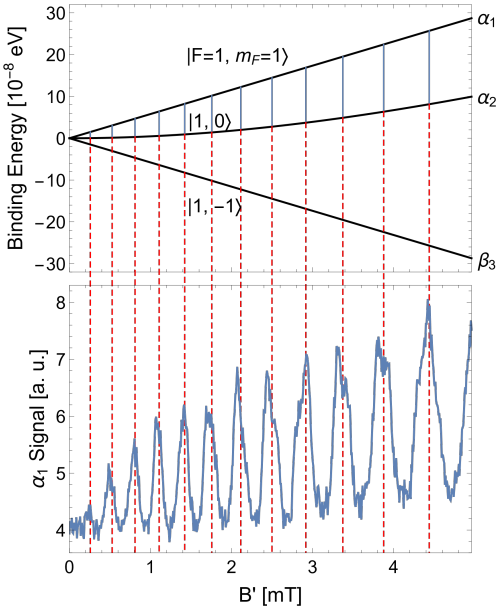

Figure 2.14: α_1 to α_1 spectra with Breit-Rabi diagram [F4].

This is exactly that what is discovered in the measurements in [F4]. Every time an odd multiply of the energy of the photons fits between the Breit-Rabi states of α_1 and α_2 the signal shows a peak, so the photon transitions worked and the atoms switched into the α_1 state again.
The dips or '*shoulders*' in the measured spectra are an effect of the depopulating photon transitions induced by the Sona unit:
The atom has also the possibility to make a photon transition from the α_2 state into the β_3 state after the zero crossing (Fig. 2.15, right side, red arrow down), which causes a negative influence on the measured spectra.

The position on the magnetic scale of the Breit-Rabi diagram is determined by the effective longitudinal magnetic field seen by the atoms when they passing the Sona magnetic field. For a nearly sinusodial shape of the magnetic field the value of the effective field would be $B_{eff} = B' \sim \frac{B}{\sqrt{2}}$ [9].

Fig. 2.15 shows a scheme of the photon induced transitions in the photon model and the turn of the quantization axis for the shown α_1 to α_1 case. If this transition worked on the left side of the zero crossing, a second photon transition on the right side of the zero crossing is very likely with symmetric fields.

This case equals to the graph in fig. 2.14 which peaks are at every crossing point of the Breit-Rabi diagram where an odd multiple of the photon energy fits between the energy levels of the α_1 and α_2 state. Again the β_4 state is not marked because it is non likely that it joins the photon induced transitions from its energy level.

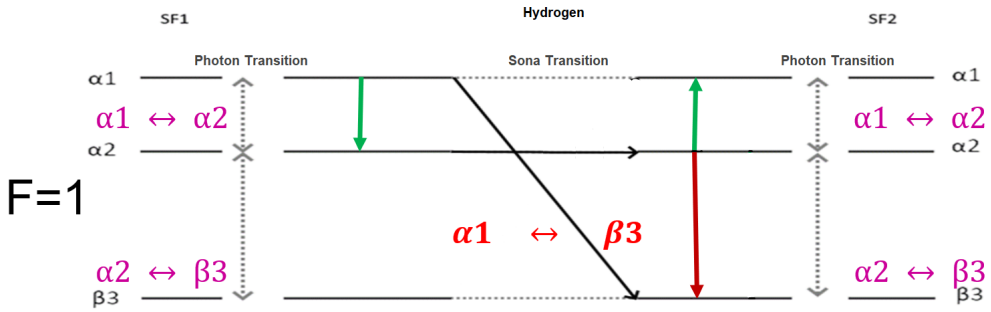

Figure 2.15: Sona transitions by longitudinal and radial magnetic fields [P1].

The energy of the photons $\Delta E_{ph} = h \cdot f$ depends on the frequency $f = \frac{1}{\Delta t}$ of the electromagnetic wave and, therefore, on the seen wavelength. This is related to the velocity of the incoming atoms and the distance between the magnetic coils with the time of flight trough the coils $\Delta t = \frac{\lambda}{v}$ [5]. The atoms pass the Sona unit with a known velocity v_{WF} depending on the set acceleration voltage inside the source and the fields inside the Wienfilter. λ is twice the distance between the centers of the magnetic coils (Compare fig. 2.16).

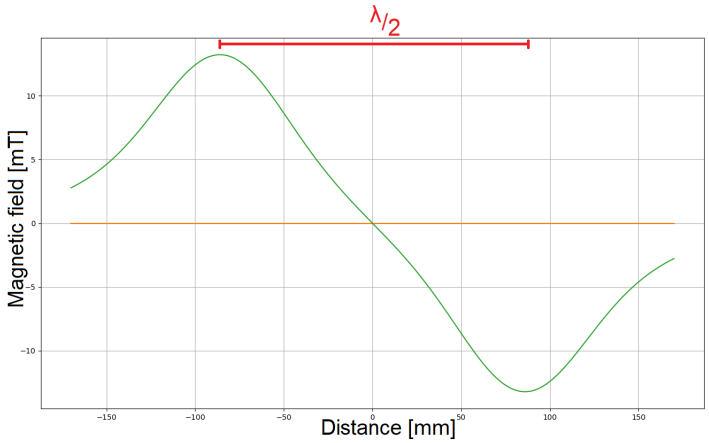

Figure 2.16: Longitudinal magnetic field with wavelength.

Tha radial magnetic field along the z-axis that is responsible for the photon induced transitions can be calculated with Gauss' law for magnetism

$$\vec{\nabla} \cdot \vec{\mathrm{B}} = 0 \tag{2.7}$$

as shown in [8] to

$$\mathrm{B_r} = -\frac{r}{2}\frac{\partial \mathrm{B_z}}{\partial \mathrm{z}}. \tag{2.8}$$

With a magnetic field in a perfect sinusodial shape the derivation of it would be a cosine and, therefore, the wavelength of the radial field should be the same.

With an acceleration voltage of about 1.5 keV the velocity of the particles can be determined as

$$\mathrm{v_{H^+}} = \sqrt{2 \cdot \frac{e\,U_B}{m_p}} = 5.4 \cdot 10^5\,\frac{\mathrm{m}}{\mathrm{s}} \tag{2.9}$$

and with the distance between the coils of 12 cm the time of flight through the Sona unit is given by

$$\Delta t = \frac{\lambda}{\mathrm{v}} \sim 4,4 \cdot 10^{-7}\,\mathrm{s}. \tag{2.10}$$

This leads to a frequency of the electromagnetic wave seen by the atoms of

$$f = \frac{1}{\Delta t} \sim 2.25\,\mathrm{MHz} \tag{2.11}$$

and finally the energy of the photons can be calculated as:

$$\Delta \mathrm{E_{ph}} = h \cdot f = h \cdot \frac{\mathrm{v}}{\lambda} \sim 9\,\mathrm{neV}. \tag{2.12}$$

It has to be mentioned that the velocity of this experienced electromagnetic wave is not the speed of light but the velocity of the particle in the laboratory frame [5] which allows to reach these small photon energies. Every time an odd multiple of this photon energy fits between the energy levels of the different Breit-Rabi states

$$\Delta \mathrm{E_{HFS}}(\mathrm{B_{eff}}) = (2n-1) \cdot \mathrm{E_{ph}} \tag{2.13}$$

a photon induced transition is possible as seen in fig. 2.12.

It has to be noticed that the photon model is a possible way to understand the induced transitions by the radial magnetic field but does not explain all observations in full detail because the interactions inside the Sona unit seems to be much more complicate and complex.

2.5 Wave Model

Another method to describe the oscillations inside the Sona unit is the use of the *wave model* which is a mathematical description of the behavior of the Breit-Rabi states. Therefore, the Schrödinger equation

$$\mathrm{H}(\vec{r},t)|\Psi(\vec{r},t)\rangle \;=\; i\hbar\frac{\partial|\Psi(\vec{r},t)\rangle}{\partial t} \tag{2.14}$$

is used [7].
The movement of the particle is described with the time and position dependent wavefunction

$$\Psi(\vec{r},t) \tag{2.15}$$

and Hamiltonian operator

$$\mathrm{H}(\vec{r},t) \;=\; \mathrm{H}_0 + \mathrm{V}(\vec{r},t). \tag{2.16}$$

The unperturbed Hamiltonian itself

$$\mathrm{H}_0 \;=\; A\vec{I}\cdot\vec{J} \tag{2.17}$$

is time independent, while the potential

$$\mathrm{V}(\vec{r},t) \;=\; -\mu_{atom}\cdot\vec{\mathrm{B}}(\vec{r},t) \;=\; -(g_j\mu_{\mathrm{B}}\vec{J}+g_I\mu_N\vec{I})\cdot\vec{\mathrm{B}}(\vec{r},t) \tag{2.18}$$

is determined by the magnetic moments of the atom and the external magnetic field and is time depending. So the interaction with the magnetic field is considered as a time depending perturbation [7].
For more informations about the derivation and the theoretical correlations visit [7] or [8].

Based on these formulas the occupation numbers of the different Breit-Rabi states while interacting with the longitudinal and radial magnetic fields of the Sona unit can be calculated [7],[8]. This allows to perform computer simulations about the 'oscillations' between the Breit-Rabi states.

Some simulations of the occupation numbers of single hyperfine substates within the Breit-Rabi diagram are shown in fig. 2.17 for unpolarized Hydrogen atoms passing a Sona unit with increasing longitudinal magnetic field amplitudes.
The relative occupation number of the α_1 state is named $|\mathrm{c}_1|^2$ here, this of the α_2 state is named $|\mathrm{c}_2|^2$, for the β_3 state $|\mathrm{c}_3|^2$ and the occupation number of the β_3 state is marked as $|\mathrm{c}_4|^2$. Additionally the polarization along the beam axis is shown which can be calculated for zero fields with

$$\mathrm{P}_\mathrm{z} \;=\; \alpha_1 - \beta_3 \tag{2.19}$$

and for high fields with

$$\mathrm{P}_\mathrm{z} \;=\; \alpha_1 + \beta_4 - \alpha_2 - \beta_3 \tag{2.20}$$

because the behavior of the Breit-Rabi states is changing for different magnetic fields [7]. This dependence can be seen in formula 2.3 which is determined by the external magnetic field.

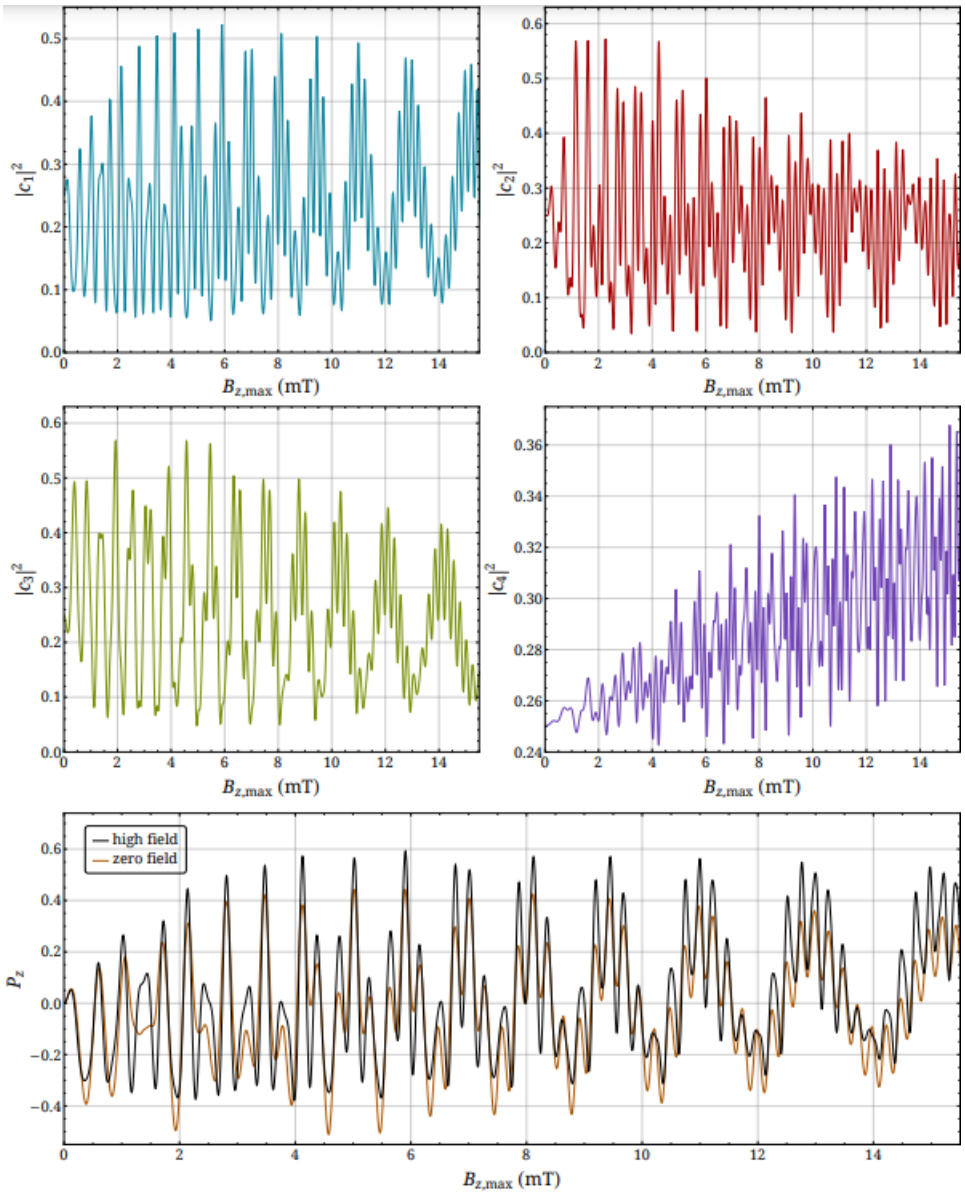

Figure 2.17: Simulations of the occupation numbers of the hyperfine states for an unpolarized beam passing a Sona transition unit and increasing the magnetic field amlpitudes [P2].

The probability for each atom to be in a state depends on the occupation numbers of the other states. For example the occupation numbers of the α_1 and β_3 state are coupled by the turn of the quantization axis which results in a minima for the α_1 state while the β_3 state has a maxima and vice versa.

The simulations also predict a larger range of the oscillations and, therefore, more particles that take part in the photon transitions if the radial offset from the center of the coils to the edge is incresasing. The radial magnetic field is rising with higher radial offsets and, therefore, more photons can be absorbed by the atoms. This can be seen in formula 2.8 for the radial magnetic field which is increasing with higher radial distances due to the $\frac{r}{2}$ factor.
Fig. 2.18 shows the simulation of the occupation numbers for the α_1 to α_1 filtered case for different radial offsets from the beam axis. Usually the graphs are on the same value at the beginning but were shifted up and down to show the individual behavior more detailed.

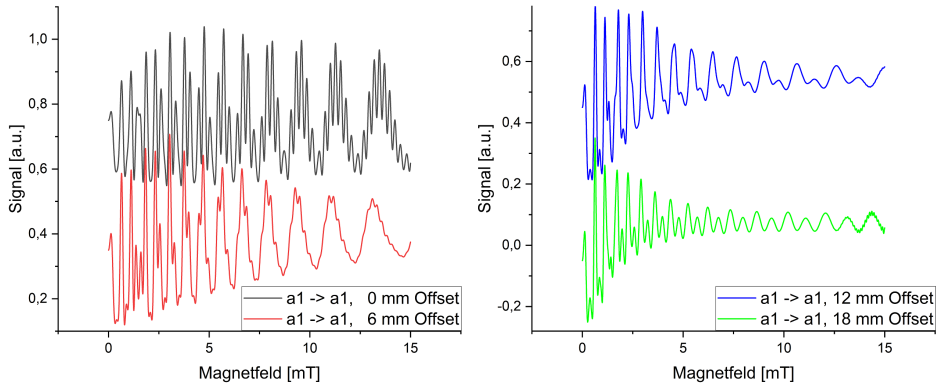

(a) (b)

Figure 2.18: Simulations for different radial offsets [P2]. Graphs are shifted in y-direction.

The amplitudes of the oscillations are rising with higher radial offsets — especially at the beginning. Also an increase of the baseline is clearly visible for higher radial offsets. In this thesis the *baseline* is defined as the connection line between the local minima of the graphs. All of this indicates that much more particles take part on the interactions when the atomic beam is off axis and higher values for polarization become possible.

3 Experimental Setup

Figure 3.1 shows the experimental setup. Fed with H_2 molecules the source will deliver H^+, H_2^+ and H_3^+ ions and accelerate them. The Wienfilter is cleaning the beam from heavy ions and sharpening the velocity distribution from the choosen mass. The next step is the caesium cell where the metastable hyperfine states will be produced by interactions with the caesium vapor. In the following spin filters different hyperfine states can be selected to produce a beam of metastable atoms in a single hyperfine substate (α_1 or α_2), in both alpha states equaly occupied or even an unpolarized beam. Between the first spin filter ('polarizer') and the second spin filter ('analyser') the modified Sona unit is placed to induce transitions between the hyperfine states of the metastable atoms.
At the end the quenchchamber and the photomuliplier are installed to *quench* the incoming atoms into the groundstate and detect the emerging photons. In the following sections the components are described in more details.

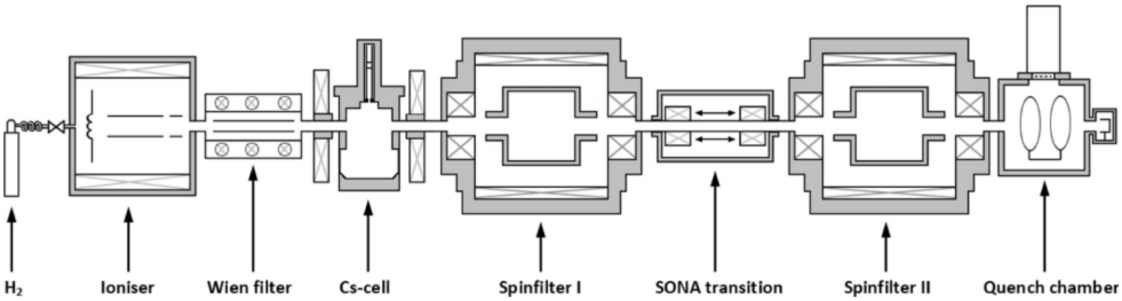

Figure 3.1: Experimental Setup [P1].

3.1 The ECR-Source

An ECR (**E**lectron **C**yclotron **R**esonance) source is used to ionize Hydrogen molecules and accelerate the emerging protons (H^+), H_2^+ and H_3^+ ions into the direction of the experimental setup.
The incoming H_2 molecules are split up into atoms and become ionized by free electrons which are forced onto circulating orbits by permanent magnets. A radio frequency is accelerating these electrons with the frequency of the circular movement so more ionisations become possible and a plasma can ignite. The emerging ions diffuse to the edge of the source where a given potential accelerates them into the direction of the experimental setup. Inside the source there is also an electrical lense to focus the ion beam to counteract the natural divergation of the beam.

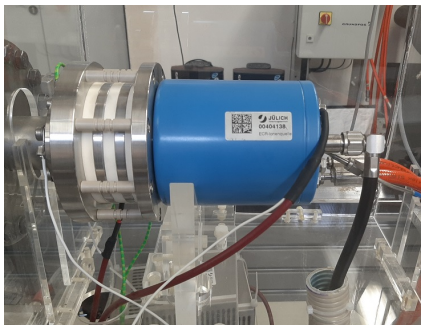

Figure 3.2: ECR ion source.

When leaving the source the potential energy of the ions equals to the kinetic energy so the velocity of the particles can be calculated by:

$$\begin{aligned} \mathrm{E_{kin}} &= \mathrm{E_{pot}} \\ \frac{1}{2} \cdot \mathrm{m_p} \cdot \mathrm{v}^2 &= \mathrm{U_B} \cdot e \\ \Leftrightarrow \qquad \mathrm{v_{particle}} &= \sqrt{2 \cdot \frac{e\,\mathrm{U_B}}{\mathrm{m_p}}} \end{aligned} \tag{3.1}$$

3.2 The Wienfilter

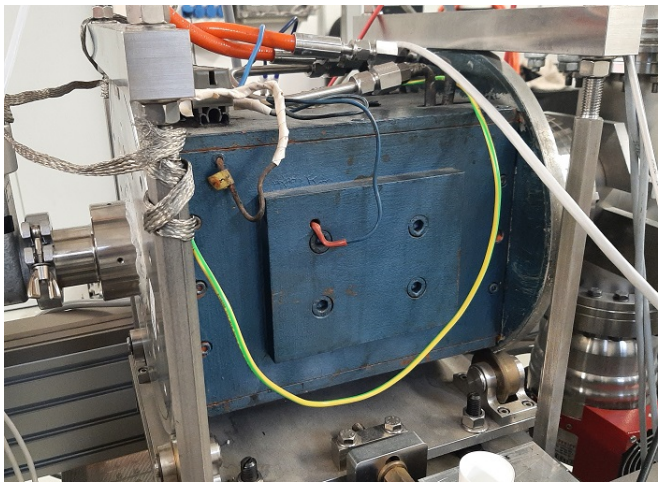

Figure 3.3: The used Wienfilter.

After the source a Wienfilter is placed which filters particles with different velocities. But due to the fact that all emerging particles are accelerated with a constant acceleration voltage, the Wienfilter is able to filter for the single masses because the velocity is determined by the mass. As an unwanted side effect the velocity of the particles is distributed even for the same mass. The reason is an inhomogneous acceleration potential inside the source which has a different influence on the acceleration of the paricles depending on their individual exact location where they were produced inside the source. Nevertheless, the velocity we want to filter can be calculated with the electrical and Lorentz force inside the Wienfilter:

$$\begin{aligned} F_{\mathrm{el}} &= F_{\mathrm{L}} \\ q \cdot E &= q \cdot v \cdot \mathrm{B} \\ \Leftrightarrow \qquad \mathrm{v_{WF}} &= \frac{\mathrm{E}}{\mathrm{B}} \end{aligned} \tag{3.2}$$

With the magnetic field perpendicular to the electric field and both to the direction of the movement.

3.3 The Caesium Cell

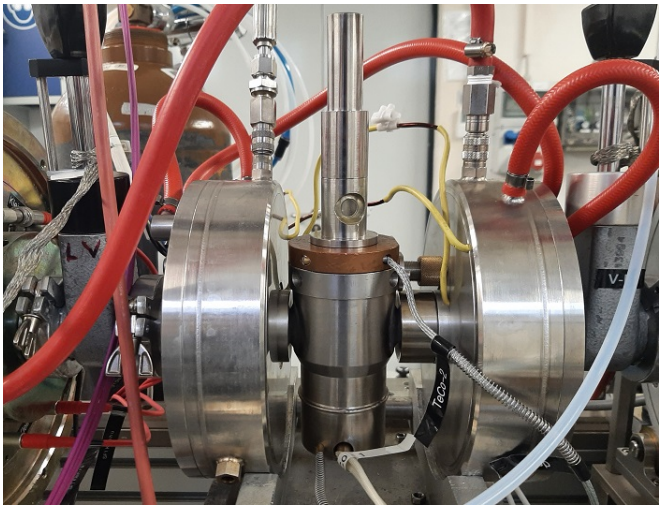

Figure 3.4: Caesium cell with water cooling tubes.

The Caesium cell is placed behind the Wienfilter. The Caesium is heated up to 160 °C until it is evaporated. The incoming Hydrogen ions react with the Caesium vapor and up to 30 % of the ions are able to switch into the metastable $2S_{1/2}$ states while the remaining atoms are in the groundstate or stay as ions in the beam [12]:

$$H_1^+ + Cs \rightarrow H_{2S_{1/2}} + Cs^+ \tag{3.3}$$

Around the Caesium cell two water cooled magnetic coils are placed to provide a longitudinal quantization axis for the emerging atoms.

3.4 The Spin filter

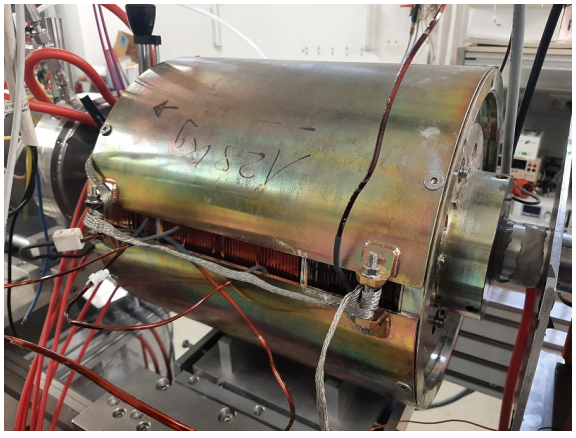

Figure 3.5: Spin filter with shielding.

There are two spin filters placed in this setup: one before and another one after the Sona unit. Each spin filter consists of five magnetic field coils around the beam axis and the superimposed magnetic fields split up the atomic energy levels of the atoms inside. The combination of electric and magnetic fields is used to reduce the lifetime of unwanted states and filter for one of two specific hyperfine states (α_1, α_2 or both).

Fig. 3.6 shows the Breit-Rabi diagram of the metastable $2S_{1/2}$ and the short living $2P_{1/2}$ states of excited hydrogen atoms with the vamous Lamb-shift in between. The crossing of the binding-energy values of the β and e-substates are marked in black.

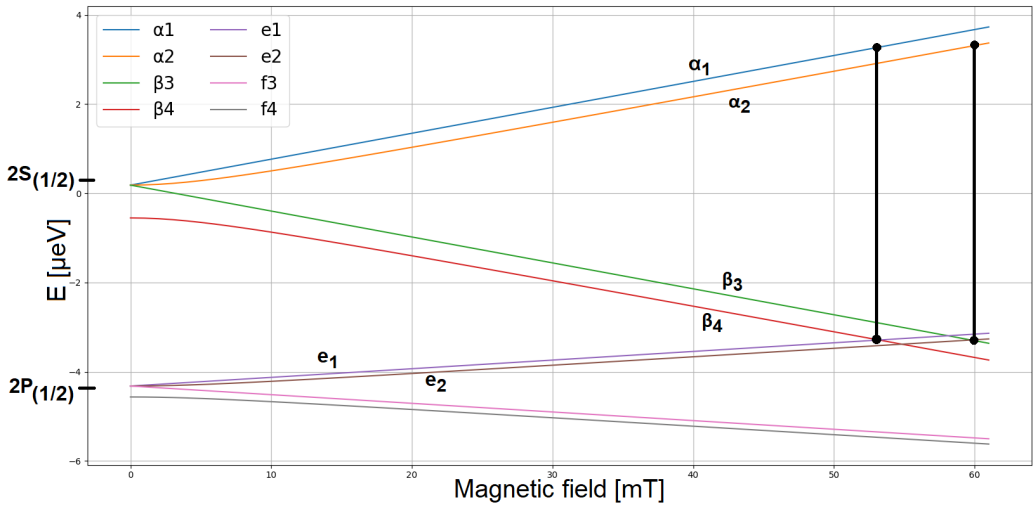

Figure 3.6: Breit-Rabi-diagramm with crossing points for the spin filter.

At an external magnetic field of about 53.5 mT (if filtering for α_1) and 60.5 mT (if filtering for α_2) the energy levels of the β and e states (from the $2P_{1/2}$ orbit) are equal. An additional electric field couples the energy levels — thus, a transition without violating the parity conservation is possible — and their lifetime will decrease rapidly. To filter for one of the alpha states a radio frequency can be used to induce oscillations between the α_1 (or α_2) and the β_4 (or β_3) state. The choosen α state is 'catched' in fast oscillations while simultaneously the other α state makes single transitions and has enough time in the β state (and, thus, the e-state) to decay into the grounstate, which results in a depopulation of the non-choosen alpha state.
Thus, a spinfilter can be used to determine which metastable alpha state is still populated or to register the number of atoms that are still in these states.

3.5 The Sona Unit

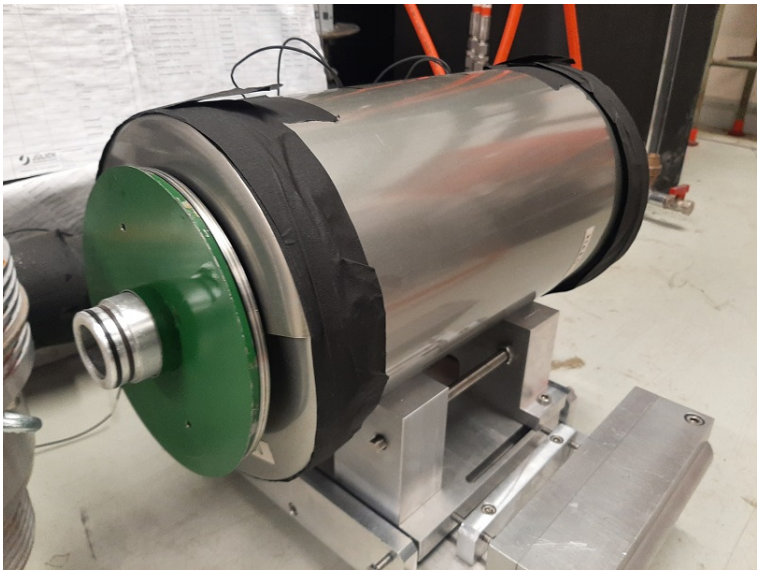

Figure 3.7: A Sona unit with magnetic shielding.

The Sona unit consists of two magnetic field coils which are operated in contrary current directions to create a zero crossing in the middle of the coils.

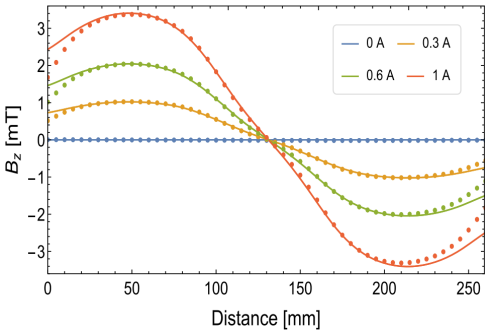

Figure 3.8: Measured (dots) and calculated (line) longitudinal magnetic field [5] for different currents send through the coils.

Fig. 3.8 shows the measured fields for the shown Sona unit. In the best case the longitudinal field is perfectly sinusodial while the fast turn of the quantization axis with the zero crossing exchanges the states of α_1 and β_3, because the precession of the spins can not follow this fast turn.
But the longitudinal magnetic field is not the only one that has an influence on the polarization. The radial magnetic field of a Sona unit is able to induce transitions between the Breit-Rabi states of incoming atoms by interactions with photons.

In this thesis this additional effect is beeing investigated: The photon transitions induced by the radial magnetic field seems to depend on the distance from the center of the atomic beam to the center of the coils due to the increasing radial magnetic field amplitude at larger radial distance r (See fig. 4.2).

3.6 The Quenching Chamber

At the end of the experimental setup the quenching chamber is placed that includes a Faraday cup to measure the intensity of an incoming ion beam and a photomuliplier dedicated to ultraviolet photons. The quenching chamber uses the first order stark effect with high electrical fields to stimulate a transition from the $2S_{1/2}$ state to the $2P_{1/2}$ state because a direct transition from the $2S_{1/2}$ state to the $1S_{1/2}$ groundstate is forbidden by the selection rules. The lifetime of the $2P_{1/2}$ state is eight orders smaller than of the $2S_{1/2}$ state. So, forcing the atoms into this state will reduce the lifetime of the atoms rapidly and 'quench' them down into the groundstate. The emitted light can be detected by the photomultiplier right on top of the quenching chamber that is able to detect and amplify even single photons. The Faraday cup is used to adjust the ion beam at the beginning before the Caesium cell is heated, so the beam can be traced and focused at the end of the experimental setup.

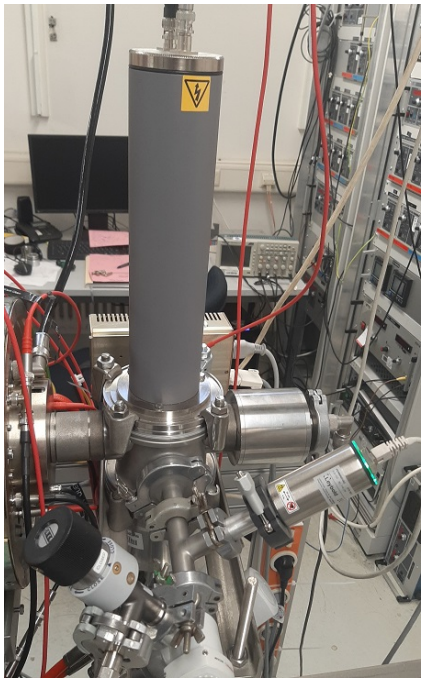

Figure 3.9: The quenching chamber with the corresponding Photomultiplier.

The measured signals from the Faraday cup and the photomuliplier are send to an oscilloscope to analyse and to store the data.

4 Measurements and Results

4.1 Adjustable Transition Unit

To investigate the radial influence of the magnetic field a new type of Sona unit was invented and build. It has two coils that can be adjusted along the beam axis for a change of the wavelength and it is also adjustable in the radial direction for a change of the radial offset.

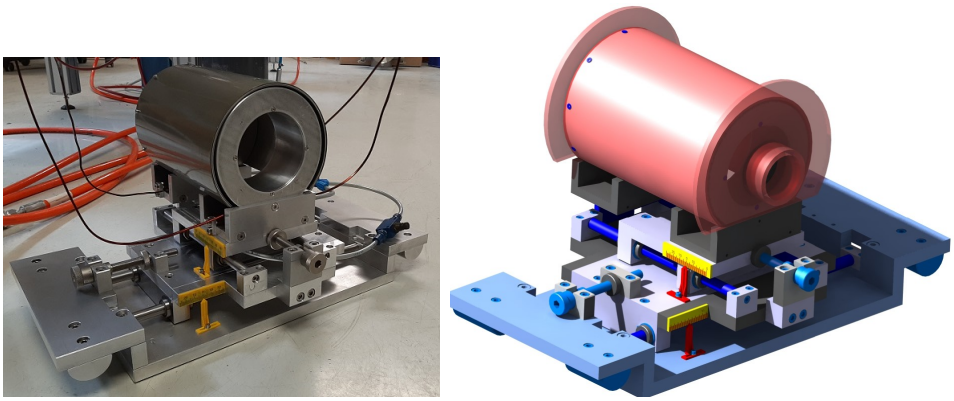

(a) (b)

Figure 4.1: New type of SONA unit [P3].

This transition unit consists of a kit of three wired magnetic coils that can be installed in the device. Two coils are wired identical and one coil has some additional windings. The coil with the additional windings allows to observe the behavior of the particles inside asymmetric shaped magnetic fields.
The specifications for the symmetric Sona setup are:

Windings per coil: $n = 140$
Resistance per coil: $R = 1.8\,\Omega$ at 24 °C

The specifications for the asymmetric Sona setup are:

Windings of symmetric coil: $n = 140$
Resistance of symmetric coil: $R = 1.8\,\Omega$ at 24 °C
Windings of asymmetric coil: $n = 171$
Resistance of asymmetric coil: $R = 2.0\,\Omega$ at 26 °C

Another parameter was not considered while planing this unit: the ratio of the diameter to the length of the coils. The diameter of the coil was doubled while the length remained the same like before. This results in stronger increasing magnetic fields in dependence of the radial offset.

4.2 Radial Influence

The simulations of the occupation numbers like shown in fig. 2.17 indicate that more particles will take part in the induced transitions and, thus, an increase of the outcoming signal seems to be possible by using a radial offset of the atomic beam instead of beeing exactly on the axis.

This can be explained by the fact that the radial magnetic field amplitude of a magnetic coil is not constant. It raises from the center — where in a perfect coil should not be any radial field — to the edge to the coil like it can be seen in formula 2.8. This behavior of the magnetic field has an influence on the experienced electromagnetic waves that are responsible for the transitions between the Breit-Rabi states. Fig. 4.2 shows a simulation of the increasing radial (orange) and longitudinal (green) magnetic field from the center ($r = 0\,mm$) to the edge ($r = 50\,mm$) of the used coils.

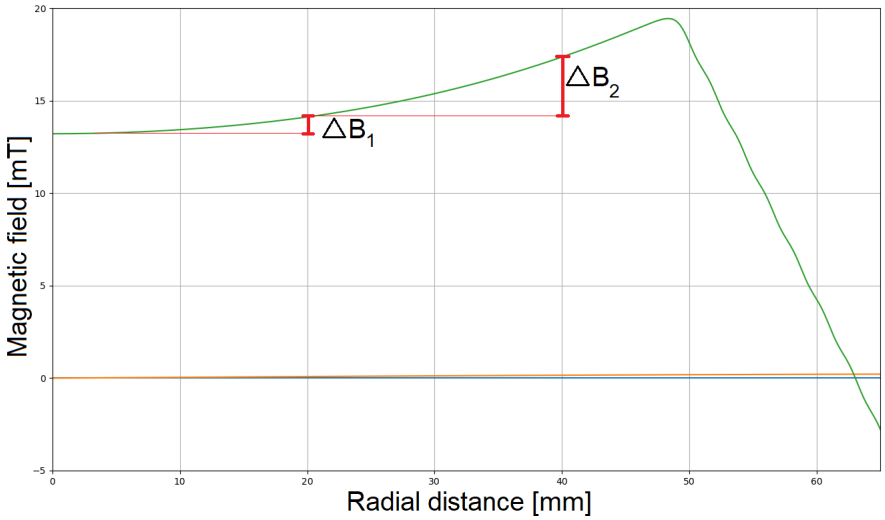

Figure 4.2: Increase of the radial (orange) and longitudinal (green) magnetic field.

The raising magnetic field in radial direction has an influence on the amount of photons that is raising with the radial distance from the center of the coil.

4.3 Influence of the Radial Distance on Polarization - Symmetric Fields

With the new type of Sona transition unit the influence of the radial magnetic field on the polarisation of the particles was investigated while the radial distance from the beam axis was increased. In this chapter the results for the symmetric magnetic coils are presented.

The measurements with this device are showing a clear visible increase of the signals and therefore more photon transitions if the radial offset is raising. Fig. 4.3 shows another measurement for the α_1 to α_1 case:

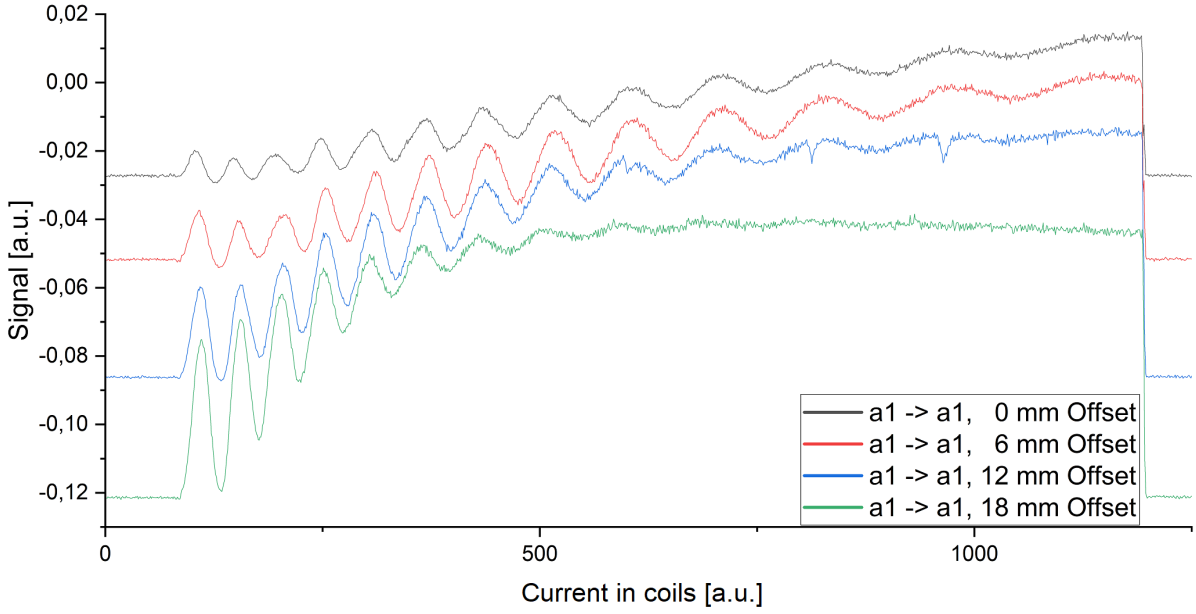

Figure 4.3: Increase of the measured signal with higher radial offsets. Graphs are shifted in y-direction.

Usually the measured signals are nearly on the same starting level, but were shifted up and down to give a better overview.

In this case only the *slow* α_1 to α_2 transition gives a positive contribution to the measured signal. At the beginning and in the middle part these *slow* transitions can be seen very well as an oscillation. These transitions are superimposed by the *fast* α_2 to β_3 transitions that can take place much more often than the slow oscillations because the distance of the energy levels is increasing faster and, therefore, the transitions can be induced much more often than in the α_1 to α_2 case (Fig. 2.11).

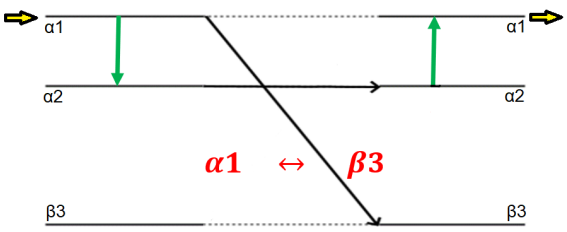

Figure 4.4: Possible transitions [P1].

It is clearly visible that a higher radial offset leads to a higher amplitude of the oscillation which means that more particles are able to make transitions. The higher the radial offset the higher the amplitude is.

At a specific magnetic field the oscillations show the appereance to stuck in a kind of saturation. This effect is not a state of totally polarization but a sequence of the circumstances of the specific experimental setup:

The atomic beam has a spatial distribution while moving along the beam axis through the experimental setup. The mentioned increase of the radial magnetic field is now causing different magnetic field amplitudes for the inner and the outer parts of the beam. If the beam is on axis the effect is neglectable for small fields but with rising magnetic fields the total difference of the field amplitudes in the innner and the outer areas of the beam increases.
Therefore, the inner and the outer part of the beam experience slightly different magnetic fields and the peaks are broadening more and more until they can be not separated anymore. So the prevailing state inside the beam is not defined anymore and the oscillations between the states can not be resolved. This effect is also increasing with higher radial offsets because the slope of the magnetic field depends on the radial offset r and is increasing for higher offsets (Compare fig. 4.2, $\Delta\,B_1$ and $\Delta\,B_2$).

It can be seen that the peaks of the measurements are shifting the higher the radial offset is (Compare fig. 4.5).

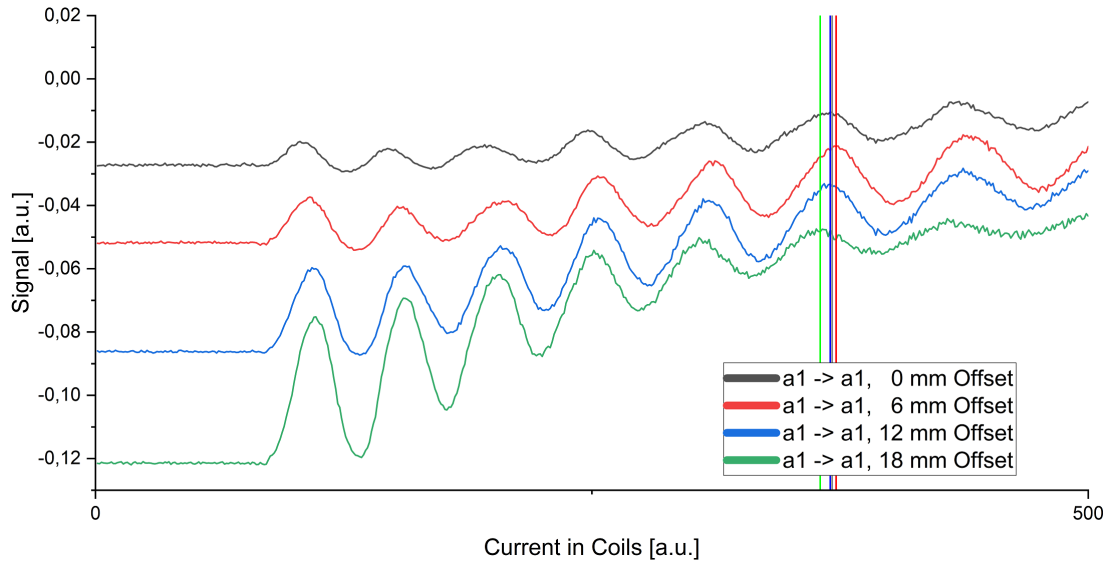

Figure 4.5: Shifting of the peaks with different offsets.

This is caused by the changing magnetic field for the same current while increasing the radial offset:
The position on the magnetic scale of the Breit-Rabi diagram describes which transition can take place and is determined by the strength of the effective longitudinal magnetic field $B_{eff} \sim \frac{B}{\sqrt{2}}$.

If the field becomes stronger due to higher radial offsets the crossing points for the Breit-Rabi state transitions are archieved for lower currents into the coils. Therefore, the transitions can take place more often and the peaks should shift to the left. The effect that the peaks are shifting to the right first can be explained by the rest magnetization of the shieldings and further external stray fields, which disturb at low currents.

The velocity of the atoms that are passing the Sona unit is not infinite sharp. The Wienfilter has a velocity distibution by the different trajectories of the particles even for the same mass. This velocity distribution results in a deviation of the experienced photon energy depending on the velocity of the individual atom.
Due to the fact that the number of absorbed photons rises by the factor of two for every photon induced transition — and therefore for every peak in the spectra — the absolute distribution of receivable energy increases. This deviation of energy is reflected by broadening oscillations in the spectra. The *fast* and *slow* oscillations run into each other and can not be resoluted anymore. It is seen very well on the width of the *slow* oscillations which is increasing for every iteration and become thicker while smearing with the *fast* oscillations.

Another pair of simulations is shown in fig. 4.6 where the raise of the magnetic field to the edge was considered.

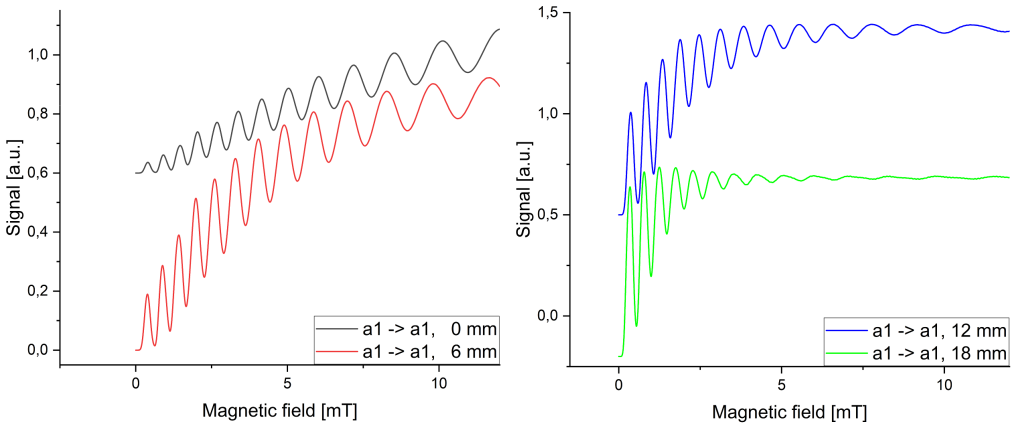

(a) (b)

Figure 4.6: Simulations with increasing radial magnetic field included [P2]. Graphs are shifted

The simulations predict a spectra that is detemined by clear visible *slow* α_1 to α_2 oscillations. Compared to the former simulations in fig. 2.18 the increase of the baseline is clearly visible more rapidly and the amplitudes of the oscillations — especially at the beginning — are not that high. Also the *point of saturation* is reached earlier and with less oscillations.

The simulations approaching ever further to the measurements from fig. 4.3. Also there is the baseline increasing more rapidly and the point of saturation is reached with less oscillations than in former simulations. The reason for this behavior is the much faster increasing radial field due to the fact that the ratio of the dimensions of the coils were not considered during the construction of this device.

For the measurements with symmetrical fields as shown in fig. 4.3 the position of the peaks can be compared to the calculated peak positions at the Breit-Rabi diagram by rescaling the measured spectra to the magnetic field. With the emerging graph it is possible to determine the effective absorbed photon energy and, therefore, with the velocity of the particles the wavelength. It works very well for the α_1 to α_1 filtered case because the peaks are representing the crossing points of the odd multiples of the slow oscillations in the Breit-Rabi diagram.

Fig. 4.7. shows the peak position of the measurements compared to the theoretical increase of the energy difference between the α_1 and α_2 energy levels for different offsets.

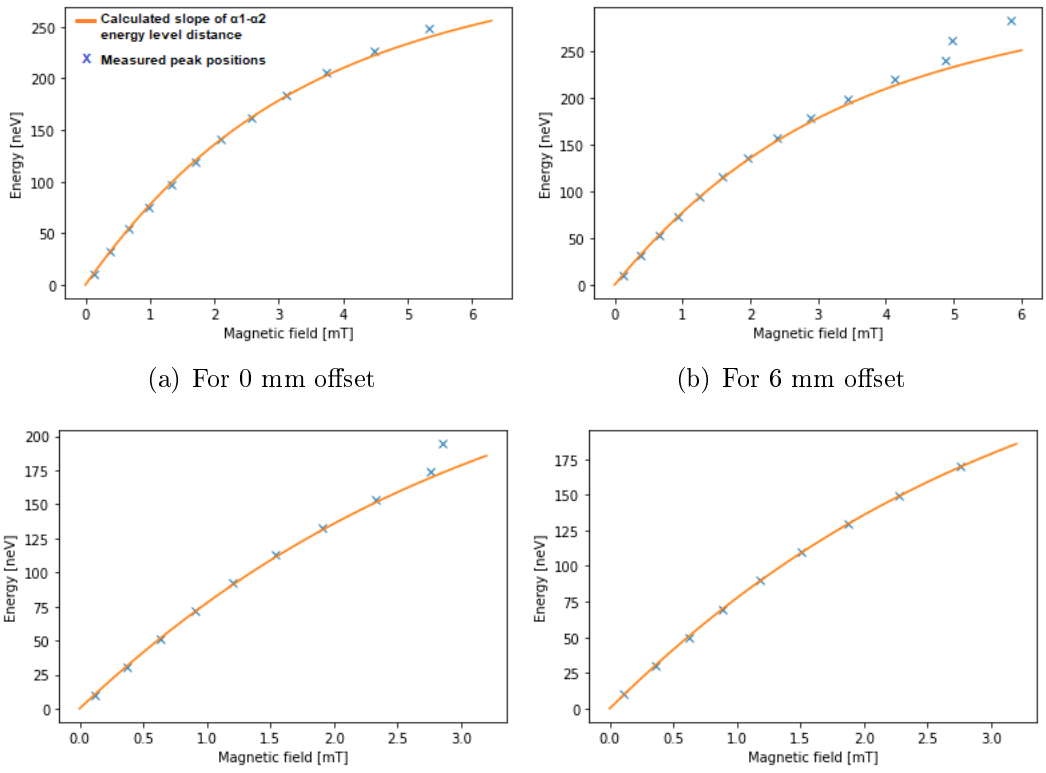

(a) For 0 mm offset

(b) For 6 mm offset

(c) For 12 mm offset

(d) For 18 mm offset

Figure 4.7: Measured peak positions compared to distance of energy levels.

To make the beginning of the measurements usable for the analysis an offset of the magnetic field was asumed because the created magnetic field of the coils will magnetize the shielding and will cause a rest magnetization even if the current trough the coils is switched off.

Fig. 4.8 shows the deviation of the measured peak positions from the calculated values.

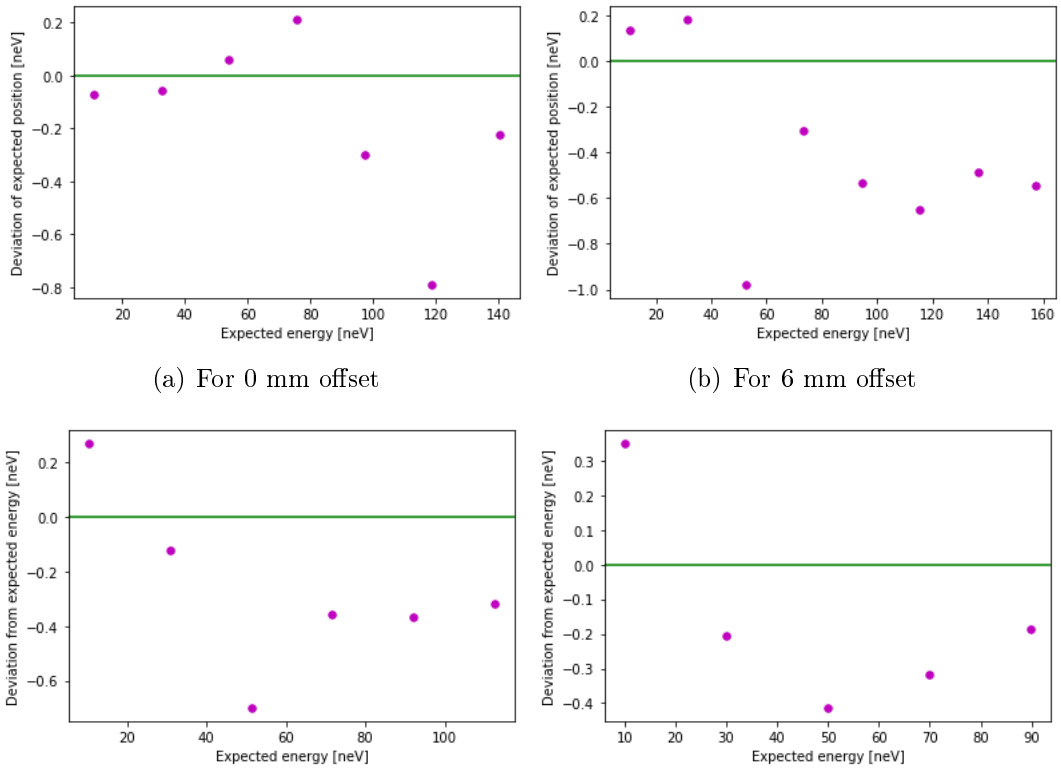

(a) For 0 mm offset

(b) For 6 mm offset

(c) For 12 mm offset

(d) For 18 mm offset

Figure 4.8: Deviation of measured peak positions compared to the calculation.

The peak positions in the rescaled spectra itself can be seen as correct in the used scale because an analysis of the peak positions with Lorentz fits showed that the uncertainty of the peak position is three up to five orders smaller than the determined peak position.

The acceleration voltage was set to 1.50 keV with an uncertainty of 0.01 keV so the velocity of the particles was calculated as $536\,064\,\frac{\mathrm{m}}{\mathrm{s}} \pm \Delta\mathrm{v} = 1.78 \cdot 10^3\,\frac{\mathrm{m}}{\mathrm{s}}$.

For the measurement with 0 mm offset a photon energy of about 10.8 neV was determined. Applying formula 2.12 this leads with the velocity distribution to the possible range of the wavelenth

$$\lambda = h \cdot \frac{536\,064\,\frac{\mathrm{m}}{\mathrm{s}} \pm 1.78 \cdot 10^3\,\frac{\mathrm{m}}{\mathrm{s}}}{10.8\,\mathrm{neV} \cdot e} = 0.2053\,\mathrm{m} \pm 0.0007\,\mathrm{m} = 205.3\,\mathrm{mm} \pm 0.7\,\mathrm{mm}. \tag{4.1}$$

While these measurements the distance between the coils was set to $\frac{\lambda}{2} = 98\,\mathrm{mm}$ what results in an expected wavelength of $\lambda = 196\,\mathrm{mm}$. The difference of the expected and the observed wavelength can be explained by the not perfect sinusodial shape of the longitudinal magnetic field.

For the 6 mm offset spectra a photon energy of 10.4 neV and a seen wavelength of $\lambda = 213.1\,\text{mm} \pm 0.7\,\text{mm}$ were determined which confirms that the wavelength is increasing with higher radial offsets.

With an offset of 12 mm the seen photon energy has changed to 10.2 neV what results in $\lambda = 217.3\,\text{mm} \pm 0.7\,\text{mm}$.
And for the measurement with 18 mm offset a seen photon energy of about 9.99 neV and an experienced wavelength of $\lambda = 221.9\,\text{mm} \pm 0.7\,\text{mm}$ was calculated.

This contradicts with the expected behavior of the magnetic field. An increase of the radial offset should change the magnetic field amplitude but not the wavelength in general.

It has to be noted that this type of analysis might work for the first peaks approximately but has some issues if its used for the whole spectra:
The measured peaks can fit for the calculated increase of the energy level distance in the beginning but because of some smearing effects with other oscillations, a velocity distribution or different experienced magnetic fields depending on the trajectories of the particles a recalculation becomes more inaccurate the higher the number of the analysed peaks is.

Fig. 4.9 shows the measured and to the magnetic field rescaled spectras with the theoretical peak position. It can be observed that with rising magnetic fields the measured peaks are shifting to the left compared to the theoretical peak position which is not an effect of a changed wavelength while increasing the current but an issue of the analysis.

The first peaks of the measurements can be seen as the most accurate ones if a rest magnetization at the beginning is considered because the effects of the possible errors have not multiplied yet and, thus, the last peaks of the measured spectras were neglected in the analysis. The issue of this method was already mentioned in former analysis like in [13].

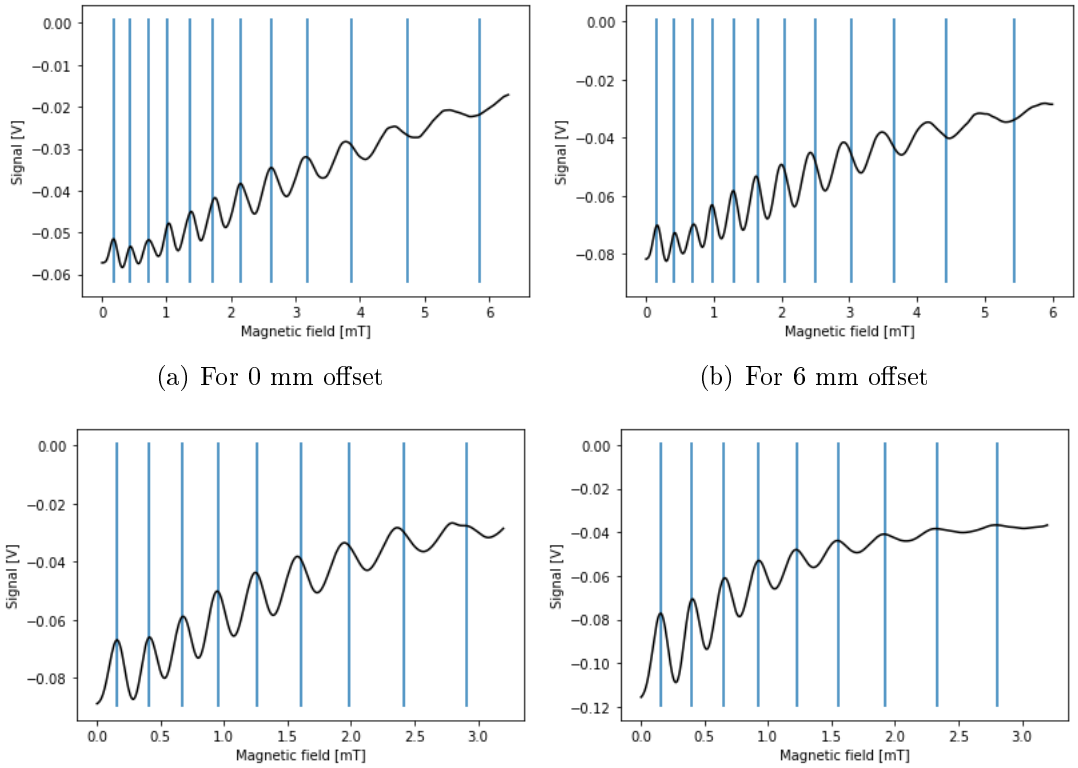

(a) For 0 mm offset

(b) For 6 mm offset

(c) For 12 mm offset

(d) For 18 mm offset

Figure 4.9: Measured peak positions compared to theoretical peak position.

Additionally it has to be mentioned that the accuracy of the recalculation of the experienced wavelength is limited because also a tiny change of the starting conditions can cause an significant shift of the peaks and the peak positions can not be assumed as absolutely correct.

To show that the transition unit principle can be used to emerge a polarized particle beam from an unpolarized beam the magnetic and electric fields of the first spin filter were turned off and just a small magnetic field inside the filter was used to provide the quantization axis for the atoms. But the measurements with an unpolarized particle beam turned out to be more difficult to realize due to the fact that a tiny electron polarisation can not be prevented by quenching the β states down with a combination of magnetical and electrical fields — induced by the magnetic fields.

Thereby, the atomic beam is basically always polarized for a small part if used in our experimental setup. The switch off from all magnetic (and therefore electric) fields before the Sona unit means a loss of the quantization axis, and thus, the Sona unit will not work like intended. With small fields applied the loss of signal intensity was too high, so a lower magnetic field strength inside the Caesium cell and the first spin filter than on normal operation were used.
But nevertheless, the measurements when an unpolarized beam enters the Sona unit and the occupation number in the α_1 substate is determined look like expected:

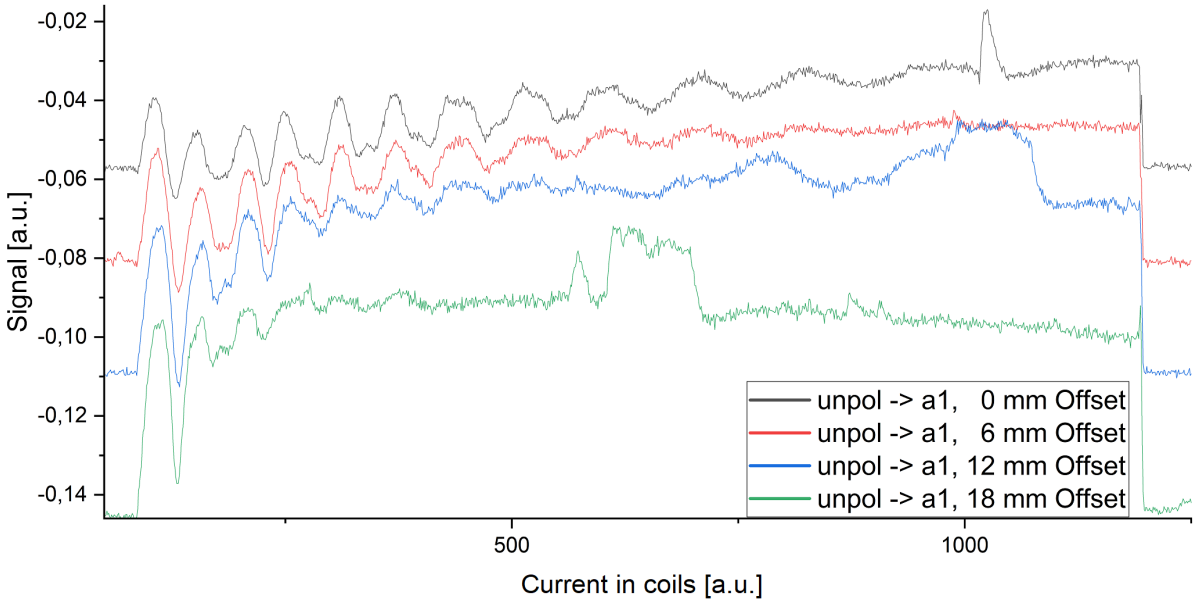

Figure 4.10: Measured spectra when an unpolarized beam enters the transition unit and the occupaion number in the α_1 substate is determined. Graphs are shifted in y-direction.

For the unpolarized to α_1 spectra an increasing signal amplitude in the begining and then some *slow* oscillations from α_1 to α_2 transitions is expected. In this spectra it is again visible that even for an unpolarized beam entering the transition unit the occupation numbers of the α_1 substate are changing when the current through the coils is increased. Thus, for some magnetic fields a polarization is produced and the amplitude of these changes can once more be increased when the radial offset between beam and magnetic field axis is increased too.

The slump and peaks of the signals at half and maximum magnetic field are not real peaks but an effect induced by the source. If the hydrogen molecule flow is not constant or the plasma inside the source changes its position the outcoming atomic beam is not stable. This causes a different amount of particles that are interacting inside the experimental setup and distort the measurements. For these measurements a more stable beam could not be established but the main structure of the signals can be seen.

Because of using the symmetric wired coils the photon energy on the left side and on the right side of the zero crossing should be the same. That means if the photon transition between α_1 and α_2 worked on the left side, a second transition on the right side is very likely. Both transitions ($\alpha_1 \leftrightarrow \alpha_2$) and ($\alpha_2 \leftrightarrow \beta_3$) can happen on both sides of the zero crossing, but can even intefere in between. Thus, depending on the strength of the single transitions at a given magnetic field amplitude, the transitions can appear at a 'one-way-street' to bring most atoms with F = 1 into a single substate with either $m_f = +1, 0$ or -1.

Also these peaks are shifted — depending on the radial offset. And also the higher amplitudes of the oscillations with increasing radial offset can be seen here very well.

The simulations for the unpolarized case are shown in fig. 4.11.

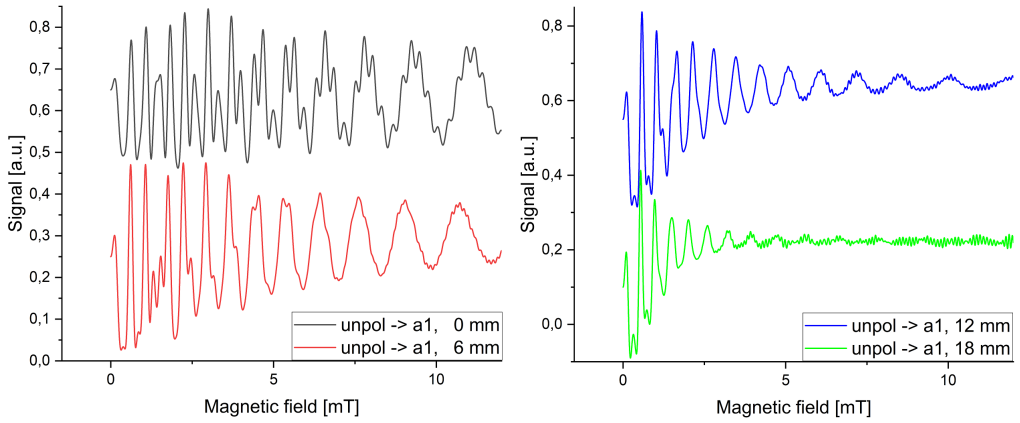

(a) (b)

Figure 4.11: Simulations with increasing radial magnetic field included [P2]. Graphs are shifted.

The main behavior of the spectra is like expected but it can not be compared exactly with the measurements. It is nearly impossible with the experimental setup to provide an unpolarized particle beam for the transition unit. Everytime a magnetic field is used it creates an electrical field in the inertial system of the particles which would reduce the lifetime of the β states so the beam becomes polarized. Due to the fact that a magnetic field is necessary to provide the quantization axis for the particles a complete unpolarized beam is not realizable and the measurements will never have the same starting conditions as the simulations. And like shown in fig. 4.12 this has an significant influence on the peak positions.
As a result the measurements for the 'unpolarized to α_1'-case look more different from the simulation than for the 'α_1 to α_1'-case.

Fig. 4.12 shows a simulation of the occupation number for the α_1 substate while the starting conditions were changed.

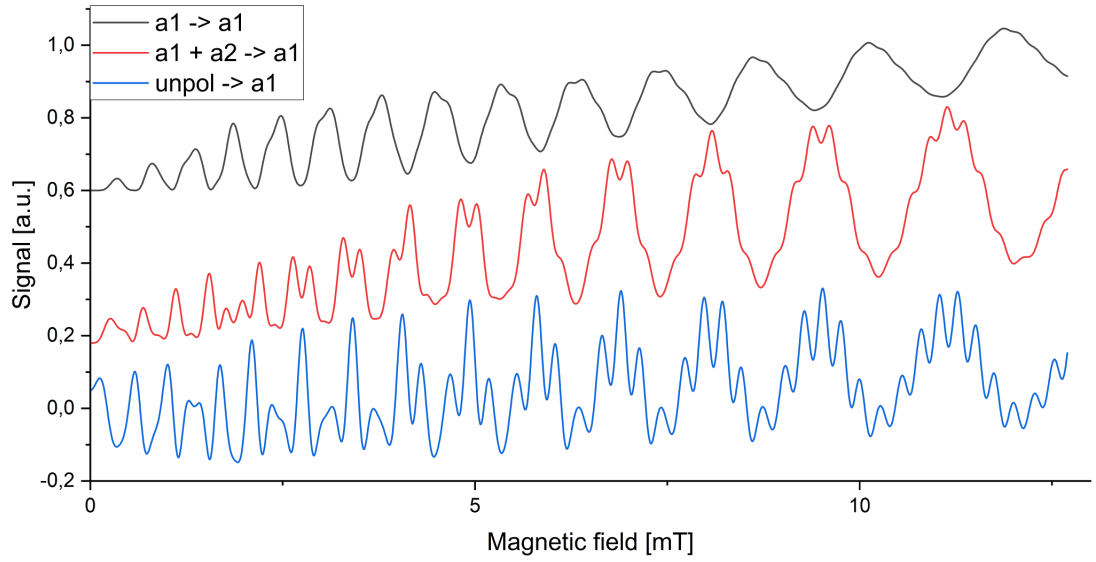

Figure 4.12: Shift of the peak positions with different starting conditions [P2].

The massive peak shifting of up to 180° phase shift while changing staring conditions can bee seen very well.
Thus it is possible that the magnetic field of the spin filter or the gradient of the magnetic field inside the Sona unit is causing a small amount of polarization and distorts the peak positions which can not be analysed in detail anymore.

The recalculation of the wavelength is only useful for measurements with a defined state inside the beam because the expected transitions can be predicted with the Breit-Rabi diagram. For example in an unpolarized case the individual peak positions can not be calculated exactly and in addition every change of the beam polarization will shift the peaks which makes an analysis of this case difficult.

4.4 Influence of the Radial Distance on Polarisation - Asymmetric Fields

The asymmetric wired coils causing asymmetric magnetic fields like shown in fig. 4.13. The amplitude of the minimum in the first coil with more windings is now larger than the maximum of the other coil. Thus, the position of the zero crossing is not in the center of the coils anymore but shifted to the lower magnetic field coil.

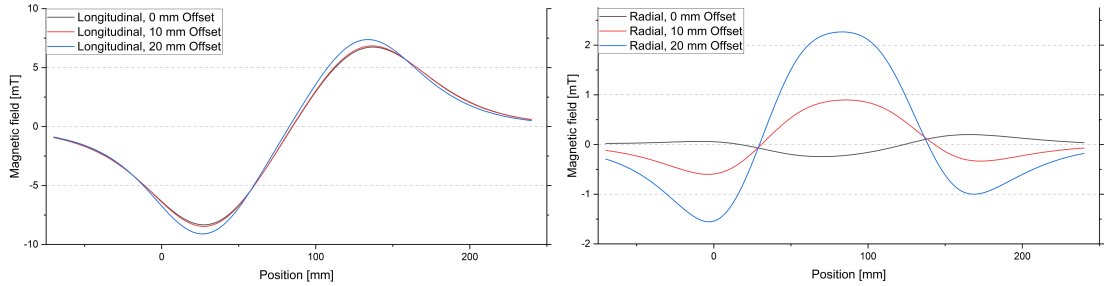

(a) (b)

Figure 4.13: Longitudinal (a) and radial (b) magnetic fields of the asymmetric Sona unit with different offsets.

It must be considered that these fields are representing the photons and an asymmetric field results in two different photon energies that are seen by the incoming atoms instead of two identical ones (Fig. 4.14).

Furthermore, this means that one of the photon transitions — before or after the zero crossing of the longitudinal field — is more likely than the other one, depending on the velocity and position of the particle inside the Sona unit. This is the reason for much more chaotic Breit-Rabi oscillations inside the Sona unit but also could be used to create polarization.

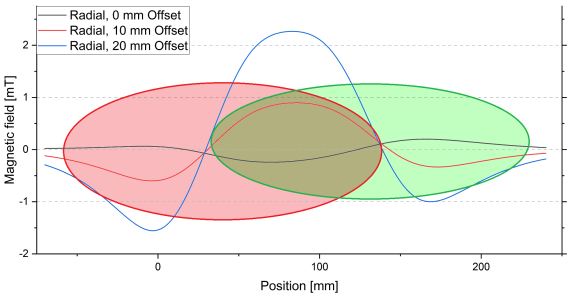

Figure 4.14: Interaction regions of the photons with different energies before and after the zero crossing.

If now metastable atoms in the substate α_1 pass trough the Sona transition with asymmetric wired coils, the occupation numbers of α_1 as function of the current through this coils is shown in fig. 4.15.

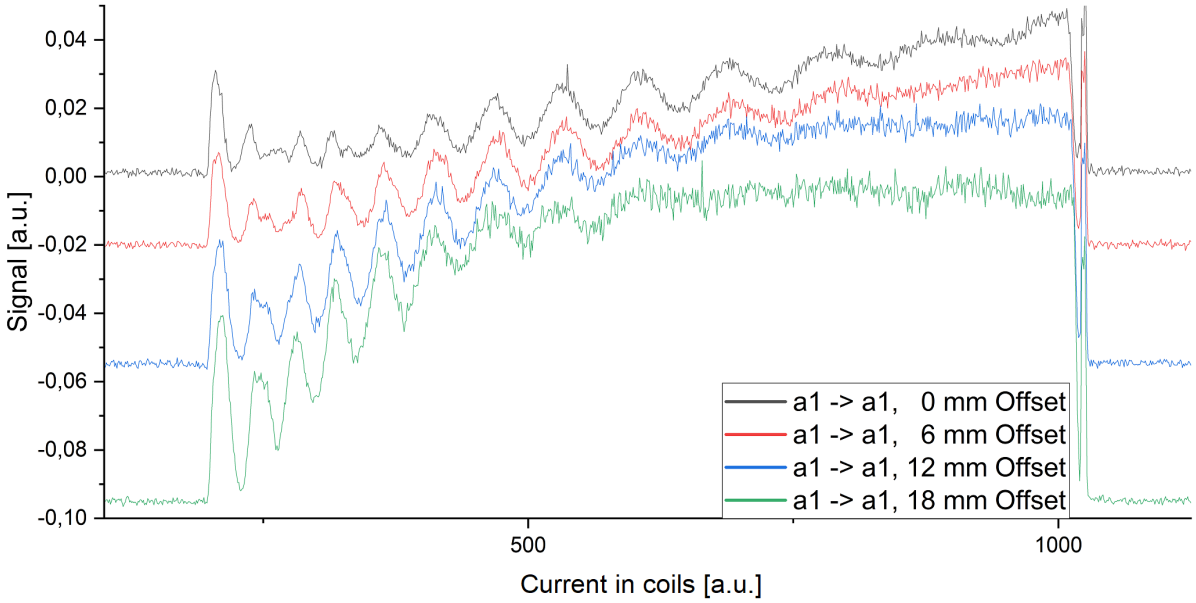

Figure 4.15: Increase of the measured signal with higher radial offsets. Graphs are shifted.

Also here an increase of the main signal is clearly visible but the structure of the oscillations looks much more chaotic than in the symmetric case. This can be explained by the inhomogeneous magnetic field that is different on the left and on the right side of the zero crossing of the Sona unit. If the photon transition worked before the zero crossing it is not likely that the same transition will also fit after it because the photon energy has changed.

Another effect of the inhomogeneous magnetic field is that with changing offset the shape of the peaks is changing instead of beeing just shifted also. The total difference between the two different photon energies on the left and on the right side of the zero crossing is increasing with higher currents trough the coils and higher radial offsets. Therefore different transitions are possible for different currents inside the coils or different offsets — which is shown by the fact that some peaks seems to split into two different peaks or two peaks will combine theirself to one peak. For example in fig. 4.15 the fourth peak for 6 mm, 12 mm and 18 mm offset is splitted into two different peaks in the spectra with 0 mm offset.

Due to the fact that the photon energy is changing asymmetrically and can not be determined exactly an analysis of this behavior with the photon modell is not an expedient solution.

The simulations for the α_1 to α_1 case with the included inhomogeneous radial magnetic field are shown in fig. 4.17.

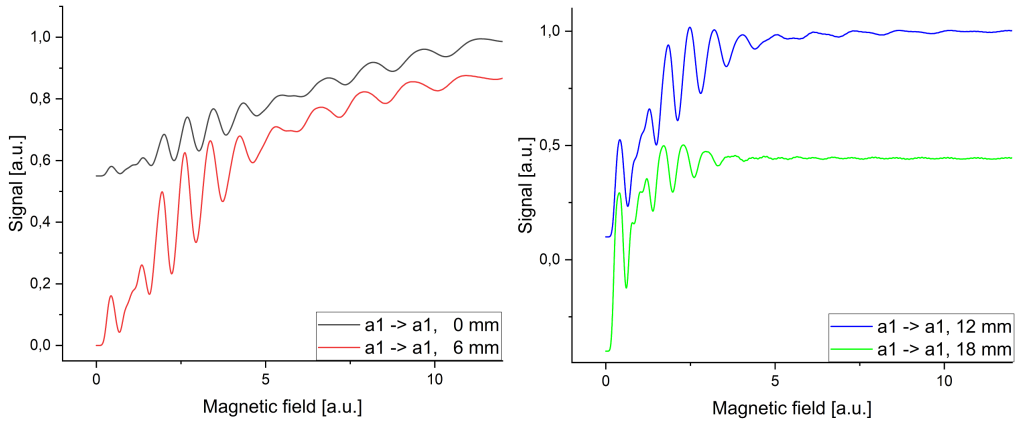

(a) (b)

Figure 4.16: Simulations with increasing radial magnetic field included [P2].Graphs are shifted

Because of the remaining rest magnetization the first peaks of the simulation can be neglected because the measurements starts already above these magnetic field values. But the simulations for this case are not fitting to the measured signal even if the main structure of the increasing baseline and the point of saturation seems similar. A possible reason for this is that the conditions of the magnetic field can not be controlled well during the experiment. The asymmetric fields are also influenced by the fields of the spin filters before and after the Sona unit, and thus, the magnetic field inside the unit must be determined approximately. This effect appears also for the symmetric case but is much more significant with asymmetric fields because the position of the zero crossing and photon energies is shifting uneven.

But also for the asymmetric magnetic field oscillations can be observed if an unpolarized atomic beam enters the Sona unit and the occupation number of the α_1 state is determined like seen in fig. 4.18.

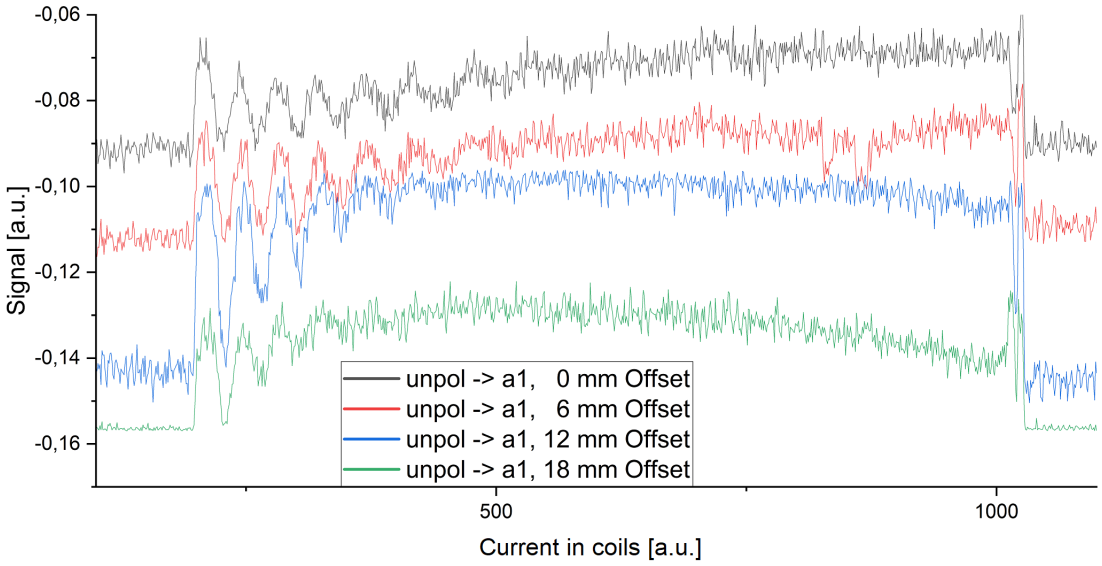

Figure 4.17: Increase of the measured signal with higher radial offsets. Graphs are shifted.

The structure of the spectra is much more chaotic than in the α_1 to α_1 case for the symmetric fields before, because much more transitions are possible inside the Sona unit and the prefered transition can not be predicted.

Another effect of the asymmetrical magnetic field is that the simulations for this case show high possible values for the polarization and the fact that the β_4 state seems to make more and stronger oscillations:

In former simulations (Fig. 2.17) with symmetric fields the β_4 state made oscillations inside the Sona unit by the hyperfine beat but came out nearly on the same level of occupation like at the start. Now the simulations are showing that it can leave the Sona unit with a significant different amount of particles than at the beginning.

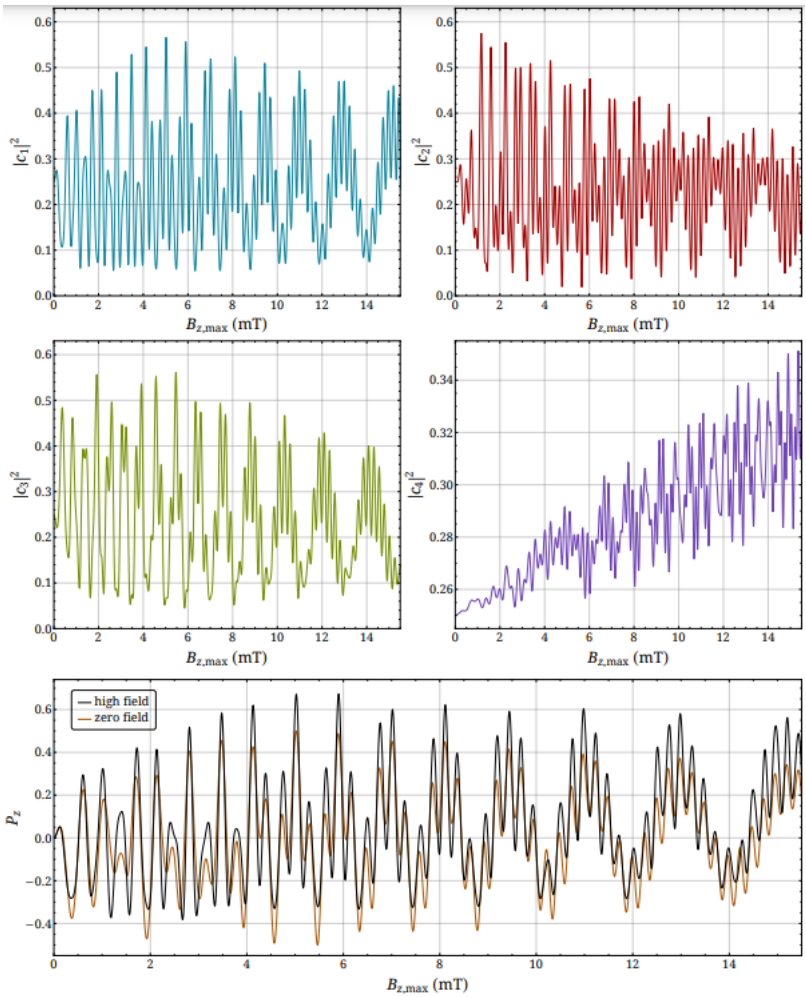

Figure 4.18: Simulation of occupation numbers for asymmetric fields [P2]. Graphs are shifted.

Fig. 4.19 shows the simulation for an asymmetric magnetic field and without the increase of the radial magnetic field for all four states and additionally the polarization of the atomic beam.
The absolute value of the β_4 state seems to stay below the value with symmetric fields (Compare fig. 2.17, purple graph) but this is just an effect of the used fields:

The asymmetric magnetic field of the Sona unit, which was used for the simulations, has a smaller magnetic field on the weaker side than the used magnetic field for the symmetric case. If the side with the lower magnetic field would have the same value as in the symmetric case the β_4 occupation number also would have a higher total amount.

Applying asymmetric fields the β_4 state has a bigger influence on the transitions and the hyperfine beat seems to become more intense. A possible reason for this behavior could be the asymmetric zero crossing between the coils. Its position is shifting to the lower magnetic field when increasing the current trough the coils. This has a big influence on the hyperfine beat which is caused by the external radial magnetic field.

4.5 Discussion of Results and Uncertainties

Even if the main principle of this transition units works there are some non neglectable systematic uncertainties for the observed wavelength and, therefore, for the experienced photon energy. These errors are propagating after every transition because the number of absorbed photons is rising by a factor of two after every transition.

The uncertainties of the measurement can be sorted by the grade they disturb the measured signal:

For the measurements with the adjustable Sona unit the increasing magnetic field for higher offsets causes the strongest uncertainty:
The longitudinal magnetc field of the coils does not depend on the radial distance until the solenoid has an infinite length. Due to the fact that the used coils are rather short compared to its diameter, there is an increase of the magnetic field strength as function of the radial distance. Thus, for the same current into the coils the metastable atoms in the beam experience a larger magnetic field if the offset gets larger. This shifts the resonances to smaller currents and is broadening the peaks in the measured spectra. This broadening smears out the peaks and the different oscillations which can not be resoluted anymore, which leads to a saturation after just a few resonances.
This error could be minimized if a small aperture is used in front of the Sona unit to reduce the spatial distribution of the beam but this would means a massive loss of intensity. Otherwise the coils need to be replaced by some coils with an increased length in relation to the diameter.

The velocity distibution of the particles is causing wider peaks after every oscillation because the distribution of the absorbed photon energy is rising for every transition. For the n^{th} peak an atom has to absorb $\sqrt{2n-1}$ photons which multiplies the error and the total amount of the deviation is increasing.
This behavior of the oscillations lead to the rising baseline of the spectra. The broadening peaks of the fast and of the slow oscillations are overlapping and the minimum of the oscillation can not be reached anymore because other transitions give allready the next positive contribution to the measured signal.

An issue for the unpolarized spectra is that we can not avoid a small amount of polarization due to the fact that every magnetic field in the experimental setup is able to reduce the lifetime of the metastable atoms in the β states rapidly. Therefore, every measurement with an unpolarized beam was not completely unpolarized. It has also been tried to implement this fact to the simulations but the grade of polarization was impossible to determine yet.

5 Conclusion and Outlook

It is found that an increase of the experienced radial magnetic field by beeing off axis has a big influence on the amount of atoms in the different hyperfine states. The number of transitions of the atoms inside the Sona unit is rising with higher radial offsets. The amplitude of the oscillations is increasing and, therefore, higher values for the beam polarization are possible.
The radial offset from the beam axis has also an influence on the amplitudes of the oscillations and therefore on the value of polarization if an unpolarized particle beam is used.

To avoid a too strong increasing magnetic field for higher radial offsets the dimensions of the coil has to be changed. Some new coil bodys have been built and are now in the coil-winding facility. The coils are twice as long as the actual ones and have the same diameter. The slower increase of the magentic field in radial direction should result in a sharper spectra and better visuable transitions.

The asymmetric solenoids could probably help to polarize some molecules that are otherwise not in range. Even H_2 and D_2 molecules or water (H_2O) show a hyperfine splitting due to the interaction of the nucleon spin alone. But this hyperfine splitting of the so-called ortho states is symmetric and might not allow to use the 'normal' Sona transition to induce polarization. But this situation might change by use of asymmetric coils to induce photons of two slightly different energies. Thus, the transition probability on both sides of the zero crossing can be manipulated separately to controll the quantum inteference in between.

6 Sources and Literature

[1] P. G. Sona, 'New method proposed to increase polarization in polarized ion sources of H^- and D^-', Energ. Nucl. **14**, pp. 295–299, Jan 1967.

[2] A. Kponou, A. Zelenski, S. Kokhanovski, & V. Zubets, article, 'Sona transition studies in the RHIC OPPIS', 2007, AIP Conference Proceedings, Volume 980; S.241.

[3] Haken-Wolf, 'Atom und Quantenphysik', 8.Auflage, Springer-Verlag.

[4] R. M. Kulsrud, H. P. Furth, and E. J. Valeo, 'Fusion Reactor Plasmas with Polarized Nuclei', Phys. Rev. Lett. 49, 1248, 1982.

[5] R. Engels, M. Büscher, P. Buske, Y. Gan, K. Grigoryev, C. Hanhart, L. Huxold, C. Kannis, A. Lehrach, H. Soltner, and V. Verhoeven, 'Direct observation of transitions between quantum states with energy differences below 10 neV employing a sona unit', Eur. Phys. J. D, **75** (9), 257, 2021.

[6] A. Görlitz, Vorlesung 'Atomphysik', Version 2020.

[7] C. Kannis, Dissertation; 'Theoretical and experimental investigation of Sona transitions', RWTH Aachen, 2023.

[8] N. Faatz, Master-Thesis; 'Simulation of the occupation numbers of hyperfine substates passing external fields', RWTH Aachen, 2023.

[9] V.A. Sahil, Bachelor-Thesis; 'Optimization of the magnetic field configuration of a Sona transition unit', FH Aachen, Campus Jülich, 2022.

[10] W. Nolting, 'Grundkurs Theoretische Physik 3: Elektrodynamik', 10.Auflage, Springer-Verlag.

[11] L. Kunkel, Bachelor-Thesis; 'Suche nach systematischen Übergangen bei magnetisch induzierten Übergängen zwischen Hyperfeinstruktur-Unterzuständen', FH Aachen, Campus Jülich 2022.

[12] R. Engels, Dissertation; 'Entwicklung eines universellen Lambshift-Polarimeters für polarisierte Atomstrahl-Targets wie an ANKE/COSY', Universität zu Köln, 2002.

[13] H. Smitmanns, Master-Thesis; 'Measurements of Transitions between Different Hyperfine Structure Substates of Hydrogen using a Sona Transition Unit', 2022.

[$F1$] Fig.2.3; de.wikipedia.org/wiki/Stern-Gerlach-Versuch#/media/Datei:Stern-Gerlach_Experiment_de.png, Copyright: Theresa Knott, last accessed March 31, 2023.

[$F2$] Fig.2.7; de.wikipedia.org/wiki/Feinstruktur_(Physik)#/media/Datei:Wasserstoff_Aufspaltung.svg, Copyright: Ellarie, last accessed April 10, 2023.

[$F3$] Fig.2.6; https//bio.groups.et.byu.net/mri_training_b_Alignment_in_Magnetic_Fields.phtml, last accessed April 23, 2023.

[$F4$] Fig.2.13; 'Präzisionsspektroskopie der Hyperfeinstruktur des Wasserstoffs' https://www.fz-juelich.de/de/ikp/ikp-2/forschung/polarisierte-teilchen-und-ihre-moeglichen-anwendungen/praezisionsspektroskopie-der-hyperfeinstruktur-des-wasserstoffs,
last accessed August 29, 2023.

[$P1$] Private communication R. Engels, 'IKP2' at the Forschungszentrum Jülich.

[$P2$] Private communication C. Kannis, 'IKP2' at the Forschungszentrum Jülich.

[$P3$] Private communication B. Klimczok, IKP at the Forschungszentrum Jülich, Technical Services and Administration.

Acknowledgements

I would like to thank all the persons who made this thesis possible. Beginning with the whole team at the IKP-2 in the Forschungszentrum Jülich.

Especially I would like to thank Ralf Engels for his continuesly guidiance and helpful explanations in every situation I believed to be lost in details. Further Chrysovalantis Kannis for his continuesly support and performing the simulations, Nicolas Faatz for the helpful discussions in all theoretical topics, Lukas Kunkel for his support at the laboratory and the patience to answer all the questions which came up and also Simon Pütz and Tarek Ahmed El-Kordy for their assistance.

I really appreaciated to work with all of you and I learned a lot.

And last but not least I would also like to thank Professor Markus Büscher who gave me the opportunity to write this thesis in Jülich and prior made it possible for me to absolve an internship there.

Appendix

Table of Content

To show that the predicted behavior of the oscillating Breit-Rabi states can be observed also for different starting conditions the polarization of the atomic beam was changed during the different measurements. Fig. 7.1 shows the spectra for the unpolarised to α_2 setup with symmetric fields. In this case a decreasing signal for the α_2 state is expected.

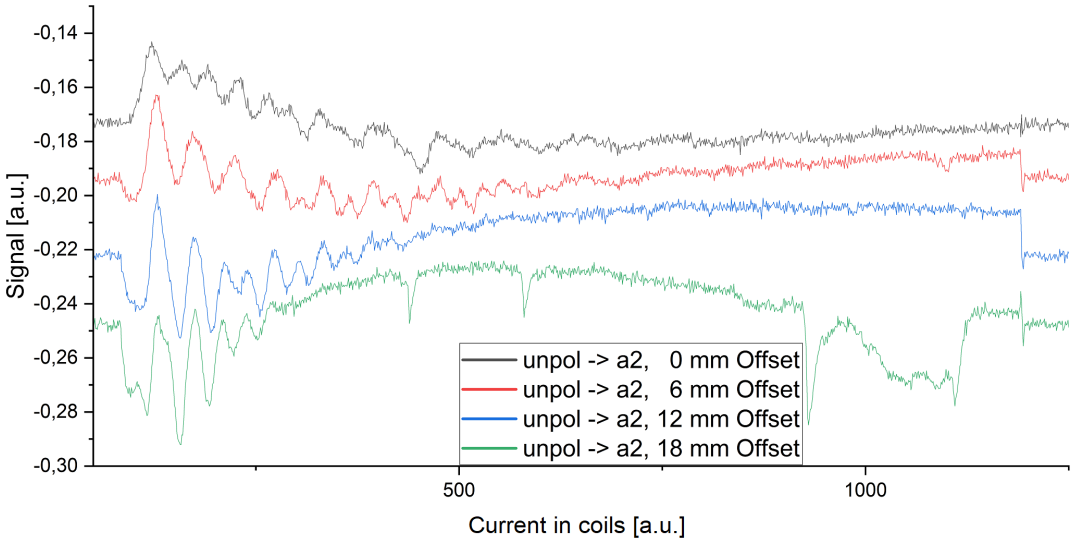

Figure 6.1: Measured spectra for unpolarised to α_2 settings.

The signal is decreasing because both photon transitions (down and up) will cause a switch into the α_2 state but used with symmetric coils the same transition is very likey on the other side of the zero crossing, and thus, the additional particles in this state will depopulate into the other states after the turn of the quantisation axis (Fig. 6.2) again.

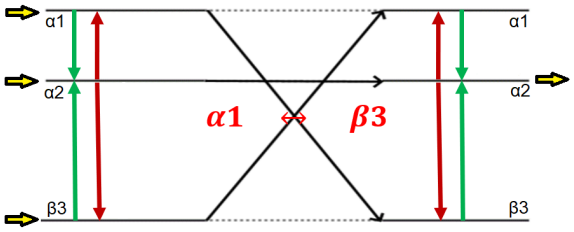

Figure 6.2: Possible transitions.

This is seen in the measurements for 0 mm offset by the decreasing signal: Every photon transition that can have a positive influence on the signal faces a transition with a negative infuence. The photon transition from α_1 to α_2 on the right side is non likely because if the photon energy would fit to this transition it is more likely that the transitions takes place on the left side of the zero crossing first and then again on the right side but into the α_1 state, and thus, it has a negative influence on the measured signal.

With higher radial offset the mentioned increase of the magnetic field and therefore the different magnetic field strenghts for the inner and outer part of the beam raises. This causes again this effect of saturation but just means that the atoms inside the beam are not in the same state.
The issues of the source for 18 mm offset at high magnetic fields can be neglected again.

To make the simulations that are shown in fig. 4.18 more comparable with them in fig. 2.17 the radial increasing magnetic field was neglected. But the simulations for the more realistic case of an increasing radial magnetic field was performed also, so here are some more simulations of the occupation numbers with used radial magnetic field inhomogenities if an unpolarized beam enters the Sona unit:
Symmetric:

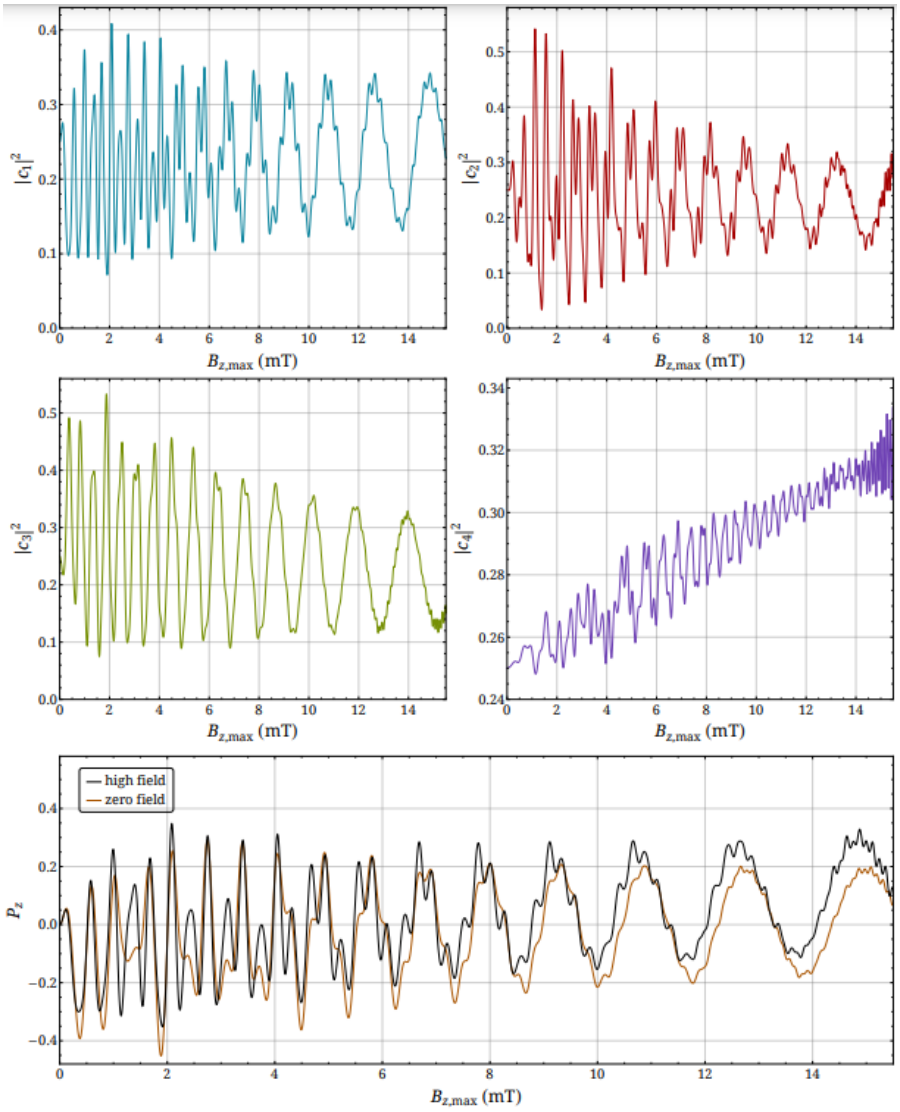

Figure 6.3: Simulation of occupation numbers for asymmetric fields.

And for the asymmetric case with field inhomogenities included.

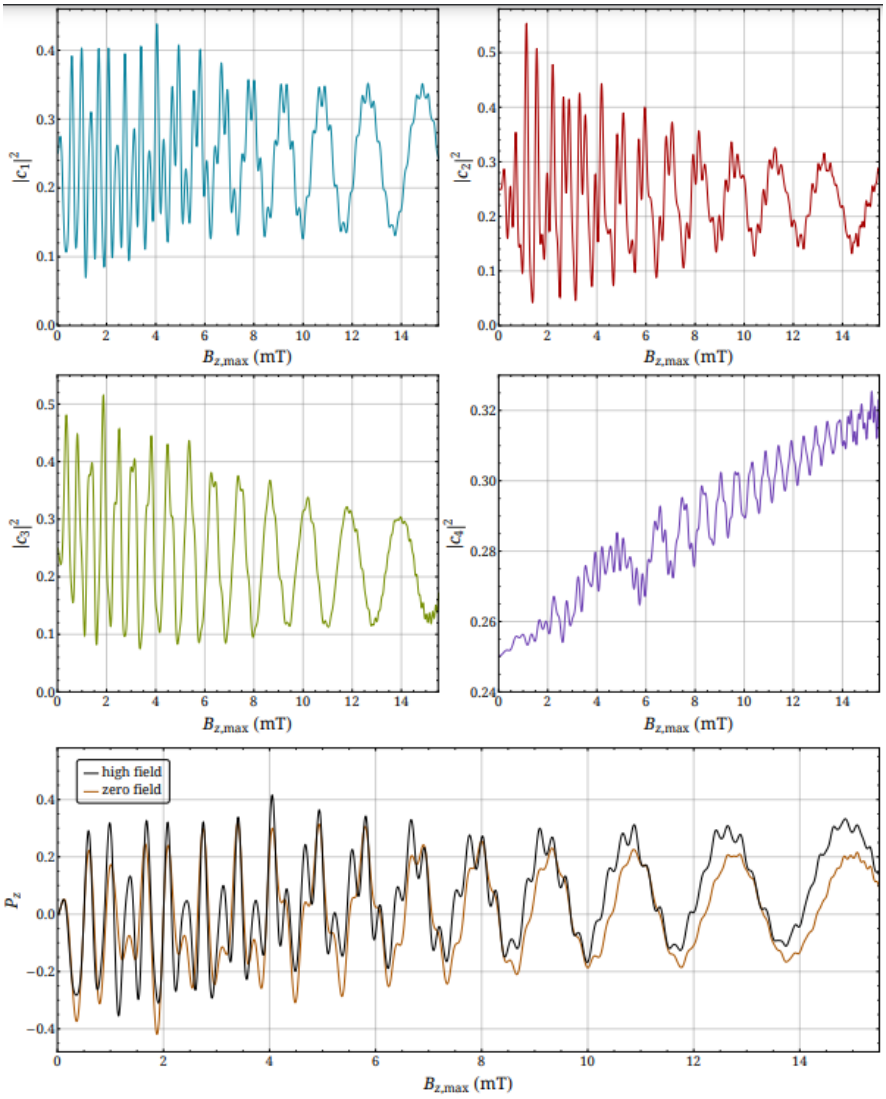

Figure 6.4: Simulation of occupation numbers for asymmetric fields.

Hiermit versichere ich, dass ich die vorliegende Bachelorarbeit selbstständig verfasst und keine anderen als die angegebenen Quellen und Hilfsmittel benutzt habe. Außerdem versichere ich, dass alle Ausführungen und grafischen Darstellungen, die anderen Quellen wörtlich und/oder sinngemäß entnommen wurden, kenntlich gemacht sind und die Arbeit in gleicher oder ähnlicher Fassung noch nicht Bestandteil einer anderen Prüfungsleistung war.

Ort, Datum	Unterschrift